nks

Nordisk kernesikkerhedsforskning
Norrænar kjarnöryggisrannsóknir
Pohjoismainen ydinturvallisuustutkimus
Nordisk kjernesikkerhetsforskning
Nordisk kärnsäkerhetsforskning
Nordic nuclear safety research

NKS-56
ISBN 87-7893-111-8

Mobile Gamma Spectrometry
Evaluation of the Resume 99 Exercise

Hans Mellander,[1)] Helle Karina Aage,[2)] Simon Karlsson,[1)]
Uffe Korsbech,[2)] Bent Lauritzen[3)] and Mark Smethurst[4)]

[1)] Swedish Radiation Protection Authority, Stockholm, Sweden
[2)] Technical University of Denmark, Lyngby, Denmark
[3)] Risø National Laboratory, Roskilde, Denmark
[4)] Geological Survey of Norway, Trondheim, Norway

June 2002

Abstract

During the RESUME 99 exercise, the radiocaesium (^{137}Cs) activity in the surroundings of Gävle in central Sweden was mapped using car-borne gamma-ray spectrometry (CGS). The CGS data along with airborne gamma-ray spectrometry (AGS) data from the same area have been used to examine possible correlations between the CGS and AGS results, detector type and position, and geographical information, such as land-use and road type. The overall differences between various CGS results are small, while larger differences are found between AGS and CGS results. In general only little correlation was found with land-use and with road-type and width. The differences between AGS and CGS results arise because airborne detectors have a different field of view than a ground-based detector. From an analysis of the depth-dependency of AGS and CGS data for a depth-distributed source, it is found that the mean mass depth may be inferred from the ratio of AGS to CGS spectral count rates.

Integration of AGS and CGS data requires a precise definition of quantities and units for reporting activity concentrations in a complicated geometry and care must be taken to translate AGS results into equivalent CGS quantities taking into account the spatial distribution of the radionuclides.

Key words

Aerial Monitoring; Cesium 137; Comparative Evaluations; Gamma Spectroscopy; Radiation Monitoring; Vehicles

NKS-56
ISBN 87-7893-111-8

The report can be obtained from
NKS Secretariat
P.O. Box 30
DK – 4000 Roskilde
Denmark

Phone +45 4677 4045
Fax +45 4677 4046
www.nks.org
e-mail nks@catscience.dk

MOBILE GAMMA SPECTROMETRY EVALUATION OF THE RESUME 99 EXERCISE

NKS
Nordic Nuclear Safety Research

Report from the BOK-1.2 project group

Hans Mellander[1)]
Helle Karina Aage[2)]
Simon Karlsson[1)]
Uffe Korsbech[2)]
Bent Lauritzen[3)]
Mark Smethurst[4)]

1) Swedish Radiation Protection Authority, Stockholm, Sweden
2) Technical University of Denmark, Lyngby, Denmark
3) Risø National Laboratory, Roskilde, Denmark
4) Geological Survey of Norway, Trondheim, Norway

SUMMARY

In the surroundings of Gävle in central Sweden many places have high concentrations of radiocaesium (^{137}Cs), stemming from the Chernobyl accident in 1986. In 1997 and 1998 the Geological Survey of Sweden mapped the area for ^{137}Cs contamination using airborne gamma-ray spectrometry (AGS), and in September 1999, the NKS exercise RESUME 99 was carried out, in which eleven teams from the Nordic and Baltic Sea countries performed car-borne gamma-ray spectrometry (CGS) in the area (Ref.1 and Ref.2).

In the present study, AGS and CGS data from the many mobile teams have been collected and are compared to each other. The data sets comprise CGS measurements taken at four calibration sites and common measurements along a 200 km calibration route. The AGS data cover a larger area, but AGS measurements taken above the same route as the CGS measurements have been selected for direct comparison with the CGS data. Possible correlations between the CGS and AGS results, detector type and position, and geographical information obtained for the area, such as land-use and road type, have been examined.

Some of the differences found between different CGS systems can easily be attributed to simple software errors, or have their origin in different calibrations. CGS results are also found to depend on detector geometry, shielding, and displacement. The overall differences between various CGS results however (disregarding software errors and different calibrations), remain small.

Larger differences are found between AGS and CGS results although the general pattern of the two data sets is similar. The differences have their origin in the fact that airborne detectors have a different field of view than a ground-based detector. For instance, a depth-distributed source may be visible to an airborne detector but may be partially shielded for the view of a detector placed on a ground-based vehicle. Also airborne measurements carried out at high travelling velocity effectively averages over larger areas than car-borne measurements. In order to integrate AGS and CGS data, care must therefore be taken to translate AGS results into equivalent CGS quantities (and vice versa), taking into account how the actual radionuclide spatial distribution (assumed or measured) will affect AGS and CGS measurements respectively.

Observed local differences between AGS and CGS could often be explained by different field of view but in several cases no obvious cause was found. In general, however, only little correlation was found with land-use and with road-type and width. From an analysis of the depth-dependency of AGS and CGS data for a depth-distributed source, it is found that the mean mass depth may be inferred from the ratio of AGS to CGS spectral count rates.
The need to compare AGS and CGS data, and to a smaller degree comparing different CGS measurements, necessitates a precise definition of quantities and units for reporting activity concentrations in a complicated geometry. Various quantities are used for reporting deposited activity concentration of ^{137}Cs. The adoption of an agreed definition will facilitate cooperation between different mobile teams in a nuclear emergency where radionuclides are dispersed in the atmosphere, with the purpose of producing a fast overview of the fallout. More specific recommendations are provided in the report.

CONTENTS PAGE

1 INTRODUCTION

In the surroundings of Gävle in central Sweden many places have high concentrations of radiocaesium (^{137}Cs), stemming from the Chernobyl accident in 1986. In 1997 and 1998 the Geological Survey of Sweden mapped the area for ^{137}Cs contamination using airborne gamma-ray spectrometry (AGS), and in September 1999, the NKS exercise RESUME 99 was carried out, in which eleven teams from the Nordic and Baltic Sea countries performed car-borne gamma-ray spectrometry (CGS) in the area (Ref. 1 and Ref. 2). Also, at the RESUME 99 exercise, seven laboratories performed *in-situ* measurements in the area and prior to the exercise the Swedish Defence Research Establishment measured the ^{137}Cs activity concentration in soil at three calibration sites.

Data from all these measurements form the basis for the work presented in this report. As part of the 1998-2001 NKS/BOK-1.2 project, "Mobile measurements and measurements strategies", the data have been analysed for the purpose of investigating how measurements from different mobile teams, car-borne and airborne and equipped with different detector systems, can be integrated to produce common and unambiguous results. The main objective of this work has been "to investigate the feasibility of integrating different field measurements, mainly (using) mobile equipment, in the early phase of a nuclear emergency situation" (Ref. 3), aiming at uniting resources and improving cooperation, nationally and internationally, following a nuclear accident.

In the present study, AGS and CGS data from the many mobile teams have been collected and are compared to each other. The data sets comprise CGS measurements taken at four calibration sites and common measurements along a 200 km calibration route. The AGS data cover a larger area, but AGS measurements taken above the same route as the CGS measurements have been selected for direct comparison with the CGS data. Possible correlations between the CGS and AGS results and detector type and position, and geographical information obtained for the area, such as land-use and road type, have been examined. Preliminary findings have been presented in the RESUME 99 exercise report (Ref. 2), which also describes the CGS equipment used and main results from the exercise.

The need to compare AGS and CGS data, and to a smaller degree comparing different CGS measurements, necessitates a precise definition of quantities and units. In the present report various quantities that can be used for reporting activity concentrations of ^{137}Cs are discussed. More generally, the adoption of an agreed definition will facilitate cooperation between different mobile teams in a nuclear emergency where radionuclides are dispersed in the atmosphere, with the purpose of producing a fast overview of the fallout.

In Section 2, mapping of large areas with AGS and CGS systems after nuclear fallout is reviewed, and in Section 3, different quantities for reporting radionuclide concentrations in the environment are examined with the emphasis on surface activity concentrations. In Section 4, the depth-dependency of AGS and CGS data for a depth-distributed source is analysed, and it is argued that the mean mass depth may be inferred from the ratio of AGS to CGS spectral count rates. In Section 5, integration of AGS and CGS measurements are discussed in terms of geographical information, including land use, road type and geometry. Sections 6 and 7 contain abbreviations and references used in the report. Finally, Appendices B and C contain definitions, a description of the analysis techniques NASVD and the "pseudo concentration method", and a description of the post-exercise processing of CGS data from RESUME 99.

2 MAPPING LARGE AREAS

Since the accident in Chernobyl in 1986 the development of mobile gamma spectrometry for environmental applications has intensified. Many European countries were affected by fallout from the accident and they have understood the need for fast mapping following such a situation. Several countries, in Europe, now have their own teams for *in-situ* and mobile field gamma spectrometry.

Satellite positioning systems and the increase in easily available computer power have facilitated rapid mapping procedures. Large data sets can be processed within a matter of seconds and data can also be processed in real time while mapping. The development of mobile communication will eventually facilitate remote real-time data processing and analysis. Very small and lightweight systems can be produced facilitating new platforms and applications. An example of a new platform is unmanned aerial vehicles (UAV's) that are being developed for military and civilian applications. Finally the growing market for geographical information systems has created a great variety of advanced software for processing and visualisation. Digital colour-shaded maps can now be produced within minutes.

Mobile gamma spectrometry measurements will produce estimates of gamma levels either as calculated dose rates or as activity estimates of individual nuclides. The source geometry is varying and mostly not known. To be able to produce the estimates, assumptions on source geometry have to be made. Errors are introduced and must be dealt with. The magnitude of the errors depends on the measurement geometry. Different platforms produce different error situations. The normal operational way to handle these problems is to have small areas or lines in common for different systems that contributes in mapping the total area. Another way is to standardize the methods to a sufficient degree to facilitate comparability. The final choice of method must depend on the task. In the table below some of the situations and solutions are described.

Table 2.1. Different tasks and comments regarding platforms, methods, products, and calibration.

Task	**Platforms & methods**	**Typical product**	**Minimum calibration**
Localizing and delineating a contaminated area or investigation of a suspected area.	All platforms can be used. Method standardisation not essential.	Binary map.	Should be focused on natural background separation.
Finding orphan sources.	All platforms can be used. Helicopters better than fixed-wing aircrafts. Method standardisation not essential.	Binary map. Table of listed sources and indications.	Should be focused on natural background separation and point source activity estimation.
Quantification of fallout or other environmental pollution.	Airborne platforms are preferred except in urban areas.	Maps displaying dose rate and/or activities.	Calibration for all expected nuclides essential. Standardisation strongly recommended.

The situation primarily discussed in this paper is a situation where large areas have been or are suspected to have been exposed to radioactive fallout or some other contamination. It can be expected that decision makers need rapid information regarding the situation. The monitoring effort must be optimised for quick and sufficiently accurate results. It is likely that this is best accomplished using a variety of systems in the air and on the ground. The needs may be different; some intermediate size areas may need a detailed investigation, some very large areas may need to be scanned in order to make a coarse estimation of the radioactivity in the area, other areas like agricultural fields may need precise measurements of nuclide composition and activity. For some measurements the primary goal may be to make dose rate estimations while other measurements can be performed to estimate the equivalent surface deposition, the equivalent surface concentration or the equivalent inventory concentration. This will involve many different types of efforts; from soil and grass sampling to *in-situ* measurements and different types of mobile measurements like airborne or car-borne gamma spectrometry (AGS or CGS). A need to integrate results from different systems, either before the last processing steps or by the decision makers or their experts arises. To be able to do this we need information regarding the characteristics of different systems and how they react to different radiation situations. Most of the work within the NKS project BOK-1.2 has been focused on these issues and especially the characteristics of car-borne versus airborne systems.

As was seen in the RESUME 99 exercise in Gävle, different measurement systems can very well be integrated and the results can be put together and compared. In Section 2.1 the benefits and drawbacks for airborne and car-borne gamma spectrometry systems while mapping large areas are discussed.

2.1 AGS versus CGS

When a platform is chosen for a survey several factors must be taken into account, i.e. area to be surveyed, expected variation, time available, cost, roads available etc. Car measurements can usually not be detailed except in urban areas. Detailed measurements are best performed with a helicopter- or with a backpack- or a terrain vehicle system if possible. Weather conditions can work both in favour and against airborne measurements. Measurement quality is usually better for airborne systems. System costs are not included but the typical airborne system is at least twice as expensive as the typical car system. Calibration costs are higher for an airborne system.

Table 2.2. Typical production rate and cost for some platforms. Costs include pilot(s), drivers and backpack carrier.

Platform	**Measurement speed (km/h)**	**Daily production (km)**	**Platform costs (SEK)**	**Production per 1000 SEK (km)**
AGS, fixed wing	250	1000	50	20
AGS, helicopter	150	600	80	13
Car	50	300	10	100
Backpack	5	20	70	14

The ability to perform fast measurements after major nuclear accidents followed by fallout or suspected fallout is of vital importance to each society. It is likely that cost will not be the most important factor when resources are deployed in the affected area. Therefore it can be expected that all available resources will be used. The question of AGS versus CGS is theoretical and of importance primarily when choosing between resources to invest in. A more fruitful approach is therefore to discuss how different types of resources should interact in a major post-accident operation.

In general, if airborne systems are available, they will play an important role after an accident. In an early phase of an emergency situation where radioactive material is involved it is hard to know the extension of the affected area. A whole country may need to be scanned in order to get a rough estimate of the gravity of the accident. In this case it is of course valuable to have access to aircrafts for rapid measurements over large areas. Airborne measurements are not limited road density and the straight flight lines are preferable for this kind of mapping. Gradually, smaller areas may be found where more detailed investigations are needed. These may be more densely populated areas like cities or places with higher activity levels. More detailed AGS measurements can now be performed with flight lines, e.g. for every 100-200 metres. In some cases this can be problematic. Tall buildings or flight restrictions may force the aircraft to fly at high altitude. Geometry effects from buildings may also cause large deviations in the results since it is mostly roofs and walls that are visible in the measurements. In a case where small areas with higher activity levels are found it can be very hard to distinguish hot particles or point sources from extended sources. Since these different source types can cause dramatic changes in dose rates at ground level it is important to combine or replace AGS measurements with other types of measurements.

The introduction of CGS measurements has one big drawback: cars can only drive on roads and therefore large areas may be left unmeasured. On the other hand cars have access to places where people spend most of their outdoor time. A large benefit is that the dose rate at ground height is obtained directly and therefore CGS measurements are valuable for dose estimations to humans. Small-scale variations in activity levels that may give large doses to small groups of the population may not be seen from an aircraft but could in many cases be identified with a CGS system. Measurements in cities are therefore more accurate using cars.

The detector systems used in cars are often smaller, cheaper and mostly they exist in more copies than does AGS systems. In most cases a CGS system can be operational long before the AGS systems and as long as the distance to the area of interest is not too large cars can start performing measurements faster than aircrafts. Since more CGS systems can be available at the same time, simultaneous measurements can be performed at different places. It was shown during RESUME 99, that if many CGS teams cooperate, large areas can be mapped as fast as when using airborne systems. Inter-calibration measurements are also important when different teams cooperate.

2.2 Possibilities with a combined utilization

As was discussed above different situations may require different types of platforms for successful and effective mapping. For mapping large-scale distribution of activity it is often better to use AGS while for estimating dose rates and for mapping small-scale variations or identifying hot spots it may be better to use CGS. Many real situations are complex and in such cases a combined use of different measurement platforms could be preferred. It was seen in RESUME 99 that it is possible to integrate AGS and CGS measurements as long as the inter-calibration between the systems is correctly performed. In RESUME 99 only CGS

measurements were included while AGS data used for comparison were obtained 2 years earlier. Because of this, AGS-CGS inter-calibration was not performed and quite large deviations between the two measurement types were observed. With the introduction of a correction factor however, good correlation was obtained.

In addition to AGS and CGS systems, in many situations other systems could be needed. In parks, along footpaths or on other open areas where cars don't have access detailed measurements could be performed with systems mounted on bicycles. Measurements in forests or other places, inaccessible even to bicycles, could be performed with the detector mounted on a backpack. An example of this kind of measurement is mapping of wetlands where fallout from Chernobyl sometimes are accumulated.

3 REVIEW OF CALIBRATION METHODS FOR AGS AND CGS

During the planning of the RESUME 99 exercise it was decided that the measured concentration of ^{137}Cs should be stated as Equivalent Surface Activity in units of Bq/m^2. Another possibility had been to state the concentration as the "inventory concentration", i.e. the total amount of ^{137}Cs found at or below the surface - integrated to a specified depth, that could be 20 cm to 40 cm. In the latter case, a calibration of the CGS equipment has to be done at a calibration site with a known inventory concentration; and the area should have a homogeneous contamination and a diameter of more than 100 m. Furthermore, one had to assume that the same relative depth distribution of ^{137}Cs was found everywhere around Gävle where the exercise measurements were going to be carried out; otherwise the words "inventory concentration" would be without sense, and a term as e.g. "Equivalent Inventory Concentration" ought to be used.

At the RESUME 95 exercise in Finland in 1995 (Ref. 4) a calibration of CGS and AGS equipment was done locally at a large lawn for which the inventory concentration was measured by extensive sampling, and horizontal homogeneity was assumed. The term "Equivalent Inventory Concentration" was, however, not used in 1995. Instead the term "activity per unit area" was used.

However, as was realized after the RESUME 99 exercise, the term "Equivalent Surface Activity" had no agreed definition. This was recognised when comparisons between the results unveiled differences that could at first not be understood. Primarily the difference was observed between Danish CGS equipment on one side and several Swedish groups on the other side. (The groups from Poland and the Baltic Countries used a calibration and definition similar the one used by the Danish Emergency Management Agency (DEMA); and the Norwegian CGS car that carried out measurements at Gävle nine months later used a definition similar to DEMA.) The two definitions are described in the following.

3.1 Definition of Equivalent Surface Concentration/Deposition

The definition of **Equivalent Surface Concentration** (ESC) used by the Danish teams is (Ref.5):

The Equivalent Surface Concentration (kBq/m^2) is that amount of true, homogeneous surface contamination per unit area that gives the same primary photon fluence rate at a certain energy at a specified height above the ground as does the actual depth distributed source. (Ref. 5 and Ref. 6).

At the field measurements by DEMA, the detector count rate - and not the fluence rate - has been used for calibration of the ESC. However, for theoretical calculations the fluence rate at first is used. Then a conversion to count rate is carried out if possible.

The definition of **Equivalent Surface Deposition** or **Equivalent Surface Activity** (ESD) used by the Swedish teams is as follows:

The equivalent surface deposition is the activity per unit area deposited on an infinite, plane surface that will produce the same primary photon fluence rate at a certain energy one meter above the surface as the actual depth distributed source. The angular distribution of the primary photon fluence from the equivalent surface deposition and the actual source can be different (Ref. 7).

The difference between the two definitions of ESC and ESD is that the ESD definition always refers to the fluence rate at 1 m height, whereas the ESC definition refers to the fluence rate at the actual detector height, even for AGS equipment carried by an aircraft at e.g. 100 m altitude. The calibration of CGS (and AGS) equipment has to be carried out in different ways according to the ESC and ESD definitions, respectively.

3.2 Calibration methods

In principle, the calibration for **ESC** of a CGS system should be carried out with the detector mounted on its car, placed in a plane area contaminated homogeneously with a true surface contamination. In practice the calibration is performed with a calibrated point source being moved around the car at distances from 0 m to 30 m or more from the detector (Ref. 8 and 9). In this way a homogeneous contamination is simulated. The detector sensitivity is the ratio between the summed full energy peak (net) count rate and the activity concentration corresponding to the simulated surface concentration.

Calibrating for **ESD** a suitable area actually contaminated with ^{137}Cs should be found. One demand on the site would be that the contamination here should be so strong that the primary photon fluence rate from ^{137}Cs could be measured without being significantly "disturbed" by the natural radioactivity. During RESUME 99 a site in Regementsparken in the town of Gävle was used. Here at first the primary photon fluence rate at 1 m height was measured with an HPGe detector with isotropic detection sensitivity for primary photons arriving to the detector "from below". The observed full energy peak count rate was "converted" to a homogeneous, true surface deposition. Next the CGS detector - mounted on the car - was placed at the same spot, and the full energy peak count rate was recorded. Finally the detector sensitivity (for ^{137}Cs) was calculated as the ratio between the CGS detector full energy peak (net) count rate and the calculated contamination concentration for the (equivalent) homogeneous, true surface deposition, ESD.

3.3 The method proposed by EU

In addition to the calibration methods for ESC and ESD also the method described in the EU Draft Standard Procedure for Deposition Mapping (Annex V) should be mentioned here (Ref. 11). The method was introduced by the Scottish AGS team and it states that the “entity” to be used for deposition mapping is **Activity per unit area,** defined as:

The activity per unit area, A_a, in Bq m^{-2}, is the activity contained in a vertical column of stated depth divided by the cross sectional area.

Activity per unit area, therefore, is the same as the Inventory Concentration used in this report. The calibration of equipment (only AGS equipment is mentioned) for measuring A_a is carried out according to the following description (Ref. 11, Section 4):

The calibration of measured spectral response, after deconvolution, can be achieved either by ground to air cross comparison or by modelling airborne detector response to a specific radionuclide (Monte Carlo approach). For the first of these, field sampling of a suitable calibration site is required, with samples being returned (normally) to a laboratory for drying, grinding, weighing, dispensing, and counting by high-resolution gamma spectrometry. The sample inventory can then be used to form calibration coefficients from the detector response at a specific altitude. A calibration site has to be chosen with care to ensure that in the ground to air comparison, a reliable correlation can be achieved. An ideal site is

approximately 500 m in diameter, relatively flat and with a relatively uniform deposition across its area and distributed in some way following recent or historical release.

3.4 Theoretical considerations for the ESC method

In Refs. 12, 7 and 5 it is shown that the fluence rate of primary photons in air at the height h_A above a plane surface contaminated homogeneously with an activity concentration q_S (assuming one photon emitted per decay in all the following calculations) is described by:

$$\varphi(h_A,S) = q_S \cdot E_1(h_A \cdot \mu_A)/2 \quad (1)$$

where μ_A is the linear attenuation coefficient of air for photons of the energy in question, and E_1 is the exponential integral of first order. "S" refers to surface and "A" refers to air. In general the activity is not found (just) at the surface; some activity has penetrated into the ground.

Assume that a horizontal layer with activity concentration $\Delta q_G(h_G)$ (Bq/m^2) is found at a depth h_G in the ground with the linear attenuation coefficient μ_G. Then one gets for the fluence rate $\Delta\varphi$ generated by this activity the expression

$$\Delta\varphi(h_A,h_G) = \Delta q_G(h_G) \cdot E_1(h_A \cdot \mu_A + h_G \cdot \mu_G)/2 \quad (2)$$

According to the definition, ESC is that true surface concentration (Bq/m^2) that generates the same fluence rate of primary photons as the actual distribution of activity, i.e. one demands that $\Delta\varphi(h_A,S) = \Delta\varphi(h_A,h_G)$ and one gets the relation

$$\Delta q_S \cdot E_1(h_A \cdot \mu_A)/2 = \Delta q_G(h_G) \cdot E_1(h_A \cdot \mu_A + h_G \cdot \mu_G)/2 \quad (3)$$

Then the Equivalent Surface Concentration corresponding to $\Delta q_G(h_G)$ becomes

$$\Delta q_S = \Delta ESC(h_A,h_G) = \Delta q_G(h_G) \cdot E_1(h_A \cdot \mu_A + h_G \cdot \mu_G) / E_1(h_A \cdot \mu_A) \quad (4)$$

Often the density of the ground ρ_G varies with the depth h_G, i.e. $\rho_G = \rho_G(h_G)$; then μ_G also becomes a function of depth i.e. $\mu_G = \mu_G(h_G)$. Therefore, one now has to replace the expression $(h_A \cdot \mu_S + h_G \cdot \mu_G)$ with $(h_A \cdot \mu_A + \Sigma\, \Delta h_G \cdot \mu_G(h_G))$, or with $h_A \cdot \mu_A + \Sigma\, (\Delta h_G \cdot \rho_G(h_G) \cdot \mu_G(h_G)/\rho_G(h_G))$.

One may define $\zeta = \Sigma\, \Delta h_G \cdot \rho_G(h_G)$ as being the intervening mass per unit area (Ref. 12) or just the mass depth. Furthermore, in general one may assume that the mass attenuation coefficient $(\mu/\rho)_G$ is a constant and Equation (4) can be replaced by

$$\Delta q_S = \Delta ESC(h_A,h_G) = \Delta q_G(h_G) \cdot E_1(h_A \cdot \mu_A + \zeta \cdot (\mu/\rho)_G) / E_1(h_A \cdot \mu_A) \quad (5)$$

The total ESC for all activity in the ground then becomes

$$ESC = \Sigma\Delta q_S = \Sigma\Delta\ ESC(h_A,h_G) \Rightarrow$$
$$ESC = (\Sigma\Delta q_G(h_G) \cdot E_1(h_A\cdot\mu_A + \zeta\cdot(\mu/\rho)_G)) / E_1(h_A\cdot\mu_A) \quad (6)$$

Here the summation should be performed for all depths with activity. Now an equivalent, mean mass depth $\zeta_{M,E}$ can be defined in at least two ways.

Case I
An equivalent, mean mass depth $\zeta_{M,E}$ can for example be found by the equation

$$[\Sigma\Delta q_G(h_G)]\cdot E_1(h_A\cdot\mu_A + (\mu/\rho)_G\cdot\zeta_{M,E}) = \Sigma[\Delta q_G(h_G)\cdot E_1(h_A\cdot\mu_A + \zeta\cdot(\mu/\rho)_G)] \quad (7)$$

Here $\Sigma\ \Delta q_G(h_G)$ is the total inventory concentration (Bq/m^2) found at or below the surface.

Case II
An equivalent, mean mass depth $\zeta_{M,E}$ can also be defined by the equation

$$ESC \cdot \zeta_{M,E} = \Sigma\ [ESC(h_A,h_G) \cdot \Sigma\ \Delta h_G\cdot\rho_G(h_G)] \quad (8)$$

In *case I* the $\zeta_{M,E}$ is that mass depth that – if all activity was concentrated here – would give the same fluence rate (at h_A) as the actual depth distribution of activity. In *case II* the $\zeta_{M,E}$ is calculated as the simple average of the mass depths with $\Delta ESC(h_A,h_G)$ as a "weight factor" for the activity at the mass depth in question.

When examining the relation between the measured spectra and depth distribution of activity, the *case II* definition is the most appropriate, and, therefore the *case II* definition of $\zeta_{M,E}$ is used in the following.

Figure 3.1 and 3.2 show how to convert a unit activity (concentration) at a specified mass depth ζ into a corresponding ESC. There are curves for h_A equal to 1.0 m, 2.20 m, and 100 m corresponding to *in-situ* measurements, CGS and AGS respectively.

Example
Assume that 500 Bq/m^2 is placed at a mass depth of 4 g/cm^2. For CGS measurements (at 220 cm) the ESC is 125 Bq/m^2. (0.25 x 500 = 125).

From Figure 3.1 it is seen that the ESC corresponding to a certain amount of activity (Bq/m^2) decreases quickly when the activity penetrates just a little into the ground – and quickest for low detector heights. For h_A =1 m a penetration from the surface to 0.5 g/cm^2 mass depth causes a reduction of the ESC to 60% of the "surface value". At 2.2 m the decrease is to 70%; and for 100-m altitude the decrease is to 93% of the "surface value". When the activity penetrates deeper into the ground the relative decrease per g/cm^2 additional mass depth is smaller; and for very deep penetrations the decrease almost follows an exponential function of $-\Delta\zeta \cdot (\mu/\rho)$. The reason is that for deeply deposited activity almost only photons moving vertically will reach the surface i.e. the attenuation then approaches that for a narrow beam of photons passing through an increasing mass thickness.

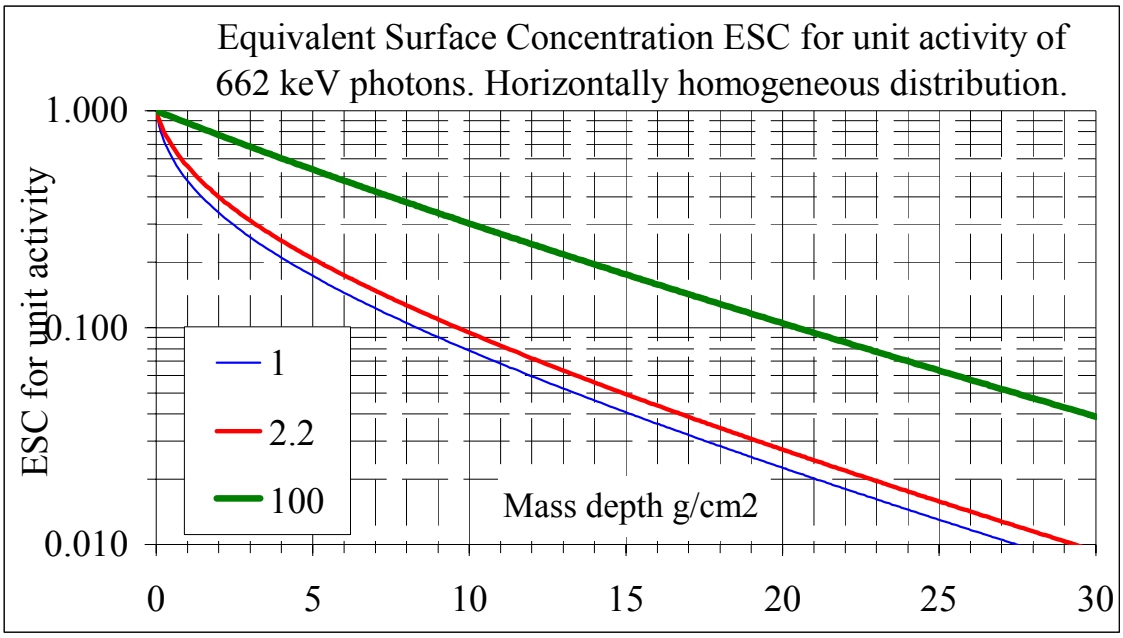

Figure 3.1. ESC for unit activity for ^{137}Cs. Mass depth 0-30 g/cm^2.

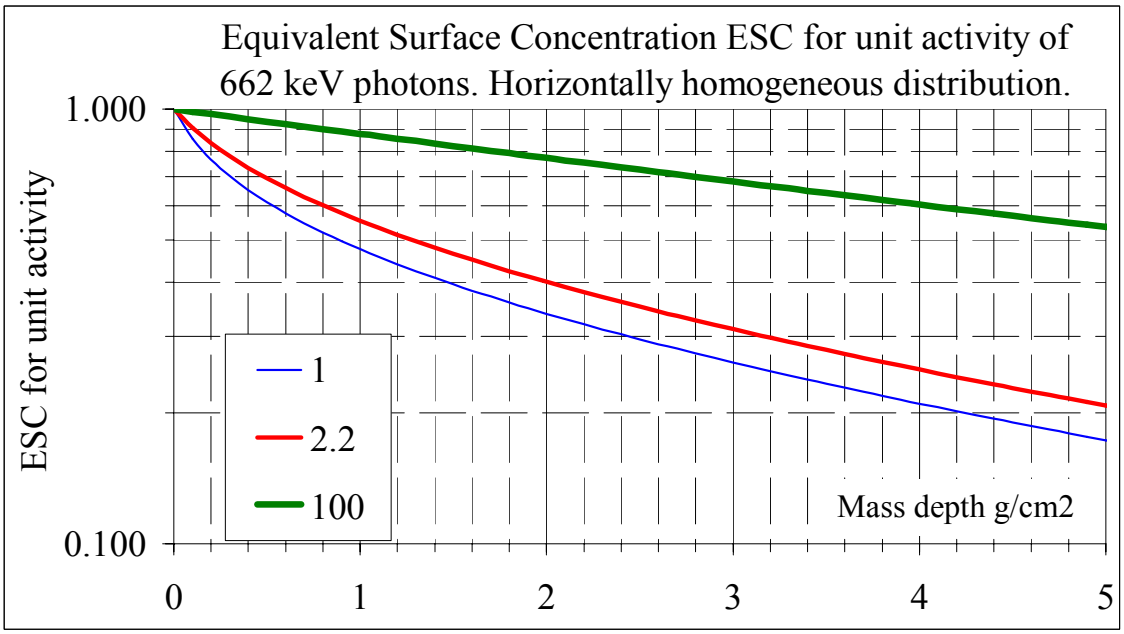

Figure 3.2. ESC for unit activity of ^{137}Cs. Mass depth 0-5 g/cm^2.

For AGS at for example 100 m altitude most primary photons arriving at the detector are moving almost vertically. Therefore the intensity versus altitude almost follows an exponential function of $(-\mu_A \cdot h_A)$. Closer to the ground the decrease with increasing altitude is faster. For large values of z (i.e. z well above 1.0) the $E_1(z)$-function itself decreases as exp(-z)/z. Here z is the mass attenuation coefficient multiplied with the total mass thickness between the activity and the detector i.e. both ground and air.

3.5 Theoretical considerations for the ESD method

3.5.1 AGS

In order to calibrate an AGS system for measuring ESD one first has to measure the fluence rate at 1 m above the ground. This is assumed done with an HPGe detector with a constant angular sensitivity (count rate per fluence rate) for photons coming from below the detector.

It is assumed that the full energy peak count rate of the HPGe detector is related to the fluence rate (ratio equal to a constant) and that the fluence rate is related to the Equivalent Surface Deposition by some (constant) calibration factor. Therefore the ESD value for any contaminated ground can be determined with the HPGe detector. This also applies to an inhomogeneously contaminated ground, but an inhomogeneously contaminated area should be avoided for calibration purposes.

The AGS (or CGS) detector is "placed" at one or several altitudes above the centre of the calibration area. For each altitude the (full energy peak) count rate is recorded. Afterwards a curve (or table) is made that relates the count rate to the ESD (determined by the “fluence rate detector” at 1m height), i.e. one now has for any altitude the relation:

$$\text{Count rate} = \text{sensitivity}(h) \cdot \text{ESD-value} \tag{9}$$

The basic formula for the fluence rate is

$$\phi(h_a) = q \cdot E_1(\Sigma\mu \cdot h)/2 \tag{10}$$

where q is the area activity concentration assumed homogeneous horizontally.
Then $\Sigma\mu \cdot h$ also can be written as any of the following expressions

$$h_A \cdot \mu_A + \Sigma \Delta h_G \cdot \rho_G(h_G) \cdot \mu_G(h_G)/\rho_G(h_G) = h_A \cdot \mu_A + \zeta \cdot (\mu/\rho)_G = h_A \cdot \mu_A + h_G \cdot \mu_G \tag{11}$$

Note: In the following the symbols “d” and “D” are used instead of h_G for the depth in the ground.

The relation between the ESD and the measured fluence rate $\phi(1\,\text{m})$ at 1 m for an activity at depth d can be expressed as

$$\text{ESD} = \alpha \cdot \phi(1\,\text{m}) = \alpha \cdot q \cdot E_1(\mu_A \cdot 1\text{m} + \mu_G \cdot d)/2 \tag{12}$$

The conversion factor α can be calculated from: $\phi(1\,\text{m}) = \text{ESD} \cdot E_1(\mu_A \cdot 1\text{m})/2$,
i.e. $\alpha = 2/E_1(\mu_A \cdot 1\text{m})$.

The fluence rate at 100 m (e.g. 70 m height + 30 m air equivalent aircraft body) is

$$\phi(100\,\text{m}) = q \cdot E_1(\mu_A \cdot 100\text{m} + \mu_G \cdot d)/2 \tag{13}$$

The calibration factor β for the AGS equipment now can be determined from

$$\text{ESD} = \beta \cdot \phi(100\text{m}) = \beta \cdot q \cdot E_1(\mu_A \cdot 100\text{m} + \mu_G \cdot d)/2 \tag{14}$$

The actual ESD is known from Eq. (12) and therefore β can be calculated as

$$\beta = \alpha \cdot E_1(\mu_A \cdot 1m + \mu_G \cdot d)/E_1(\mu_A \cdot 100m + \mu_G \cdot d) \quad (15)$$

We now assume that the detectors are transferred to another area where the activity is buried at the depth D in the ground, and repeat the calibration.

The new conversion factor β_{NEW} becomes

$$\beta_{NEW} = \alpha \cdot E_1(\mu_A \cdot 1m + \mu_G \cdot D)/E_1(\mu_A \cdot 100m + \mu_G \cdot D) \quad (16)$$

the ratio between new and old β becomes

$$\beta_{NEW}/\beta = E_1(\mu_A \cdot 1m+\mu_G \cdot D)*E_1(\mu_A \cdot 100m + \mu_G \cdot d)/(E_1(\mu_A \cdot 100m+\mu_G \cdot D)*E_1(\mu_A \cdot 1m +\mu_G \cdot d)) \quad (17)$$

Example
d corresponds to 0.5 g/cm^2 and D corresponds to 3 g/cm^2 and $\mu/\rho = 0.077$ cm^2/g for both air and ground. Then $\beta_{NEW}/\beta = 0.595$. Therefore, if the old calibration is used, the AGS equipment overestimates the ESD with a factor 1.68.

If count rates r are used instead of fluence rates one obtains

$$\beta_{CR} = \alpha \cdot E_1(\mu_A \cdot 1m + \mu_G \cdot d)/E_1(\mu_A \cdot 100m + \mu_G \cdot d) \cdot \eta_{HPGe}/\eta_{NaI} \quad (18)$$

where η_{HPGe} and η_{NaI} are the detector efficiencies that depend on the angular distribution of photons. The η_{HPGe} is assumed to have no angular variation, i.e. it is a constant independent of $\Sigma\mu \cdot h$. The detection probability of the AGS detector at e.g. 100 m altitude has a strong angular dependency. The flux of primary photons at 100 m altitude, however, is almost vertical and, therefore, the angular variation of the detection efficiency of the AGS detector is without significant importance.

3.5.2 CGS

Similar calculations can be done for a CGS calibration. The equations for AGS above are repeated here for CGS, with the detector at 2.2 m above the ground. As above one has

Count rate = sensitivity(h) · ESD-value and (9a)

$$ESD = \alpha \cdot \phi(1\,m) = \alpha \cdot q \cdot E_1(\mu_A \cdot 1m + \mu_G \cdot d)/2 \quad (12a)$$

The fluence rate at 2.2 m is

$$\phi(2.2\,m) = q \cdot E_1(\mu_A \cdot 2.2m + \mu_G \cdot d)/2 \quad (13a)$$

The calibration factor b for the CGS equipment now can be determined from

$$ESD = b \cdot \phi(2.2m) = b \cdot q \cdot E_1(\mu_A \cdot 2.2m + \mu_G \cdot d)/2 \quad (14a)$$

Next b can be calculated as

$$b = \alpha \cdot E_1(\mu_A \cdot 1m + \mu_G \cdot d)/E_1(\mu_A \cdot 2.2m + \mu_G \cdot d) \quad (15a)$$

If count rates r are used instead of fluence rates one gets

$$b_{CR} = \alpha \cdot E_1(\mu_A \cdot 1m + \mu_G \cdot d)/E_1(\mu_A \cdot 2.2m + \mu_G \cdot d) \cdot \eta_{HPGe}/\eta_{NaI} \quad (18a)$$

where η_{HPGe} and η_{NaI} are the detector efficiencies that are dependent on the angular distribution of the fluence of photons. The angular variation of the detector efficiencies is neglected again for a moment. The detectors are now transferred to another area where the radioactivity is at the depth D in the ground. Here the new conversions factor b_{NEW} becomes:

$$b_{NEW} = \alpha \cdot E_1(\mu_A \cdot 1m + \mu_G \cdot D)/E_1(\mu_A \cdot 2.2m + \mu_G \cdot D) \quad (16a)$$

and the ratio between new and old b becomes

$$b_{NEW}/b = E_1(\mu_A \cdot 1m + \mu_G \cdot D) * E_1(\mu_A \cdot 2.2m + \mu_G \cdot d) / ((E_1(\mu_A \cdot 2.2m + \mu_G \cdot D) * E_1(\mu_A \cdot 1m + \mu_G \cdot d)) \quad (17a)$$

Example
d corresponds to 0.5 g/cm^2 and D corresponds to 3 g/cm^2 and μ/ρ = 0.077 cm^2/g for both air and ground. One has $b_{NEW}/b = 0.95 = 1/1.05$. Therefore, if the old calibration is used, the CGS equipment overestimates the ESD with 5%.

If one instead calibrates in an area with the contamination at 0.5 g/cm^2 mass depth and then measures in an area with 0.2 g/cm^2 mass depth, then b_{NEW}/b becomes 1.08 i.e. one underestimates the ESD with 8% for the CGS system. For the AGS equipment at 100 m (equivalent) altitude the underestimation is 20 %.

3.6 Benefits and drawbacks for each method

In the following the methods are evaluated keeping in mind a situation where an area should be mapped as fast as possible after a nuclear accident occurs causing widespread contamination. One may also have in mind that different groups with different equipment have to co-operate in order to perform a mapping of a large area. Furthermore, one has to evaluate the possibility for (real-time) mapping during measurements and afterwards. Also the complexity of data handling should be included in the evaluation.

It should, however, be pointed out that the raw results, spectra and window count rates, at any time can be used for producing maps based on any calibration method if information on calibration parameters is available. Furthermore it should be stressed that the calibration methods discussed here simply differ by having different constant calibration factors.

3.6.1 The ESC method

Benefits:
The equipment can be calibrated on beforehand for generating ESC results immediately. This can be used for mapping while measuring. The maps generated can be supplemented with two colour codes; one for ESC and one for any *assumed* mean (mass) depth of activity.

Drawbacks:
Even for fresh fall-out the calculated ESC of e.g. ^{137}Cs will be significantly lower than the inventory concentration i.e. the activity actually deposited per unit area. The deficit will be larger for CGS than for AGS – and for *in-situ* measurements at 1 m height it will be even larger.

If different cars are used together with the CGS equipment one needs in principle a calibration for each car. (For detectors placed well above the roof of the car one may use same calibration for several car types because the activity deposited on the road itself is of minor importance.)

Comments:
AGS, CGS and *in-situ* equipment calibrated for measuring ESC only gives the same result for a true surface contamination. However, this calibration can easily be changed to account for a specific mean depth or depth distribution; and the results for AGS, CGS and *in-situ* will agree for a contamination at just that mean depth or depth distribution.

3.6.2 The ESD method

Benefits:
If the measurement areas have the same relative depth distribution as found at the calibration site, results from AGS and CGS fit (by definition) with *in-situ* results and can therefore easily be compared. A calibration is quick and easy to perform and will automatically contain all radionuclides of interest for the measurement.

Drawbacks:
The measured results (spectra or window count rates) cannot be processed before an inter-calibration with an HPGe detector has been carried out at a suitable calibration site. A mapping while measuring, therefore, also has to wait for an inter-calibration.

Comments:
Until a calibration has been carried out, maps based on an *assumed* depth distribution (or mean mass depth) can be made if sensitivities for the assumed distribution are available.
AGS, CGS and *in-situ* equipment calibrated for measuring ESD only gives the same results for a contamination with the same depth distribution (mean depth) as that existing at the calibration site. It is possible but somewhat complicated to change this calibration to fit another depth distributed activity.

3.6.3 The Proposed EU method

Benefits:
The CGS and AGS results (inventory concentrations) agree by definition with the amount of activity deposited if the relative depth distribution of the area to be measured is equal to that for the calibration area. The amount of activity deposited is a parameter of interest for radio-ecologists and for authorities responsible for introducing countermeasures (especially for foodstuffs).

Drawbacks:
The measured results (spectra or window count rates) cannot be processed correctly before a calibration based on sampling has been carried out at a suitable calibration site. Search for a suitable site, sampling and laboratory processing of samples may last several days.

Calibration factors may be calculated by Monte Carlo methods if the depth distribution of the activity is known. If this knowledge is to be gained by sampling, a significant delay also comes up here.

An estimate of mean (mass) depth of activity may sometimes be obtained by comparing full energy peaks of an HPGe detector with the Compton continuum. This can be done within an hour if the detector system is available at the calibration site. However, experiences until now indicate that the mean (mass) depth determined in this way includes significant uncertainty – and for spectra with gamma signals from several nuclides this uncertainty may grow further and make the method unusable.

Comments:
Until a calibration has been carried out at a suitable site, maps based on an assumed depth distribution (or mean mass depth) can be made, if calibration factors for the assumed distribution are available. Also mapping while measuring can be done based on an assumed depth distribution.

AGS, CGS and *in-situ* equipment calibrated for measuring inventory concentration according to the proposed EU method only gives the same results for a contamination with the same depth distribution (mean depth) as that of the calibration site. It is possible but somewhat complicated to change this calibration to fit another depth distributed activity. With this in mind one may refer to the proposed EU calibration as measurements of Equivalent Inventory Concentration (EIC). It should be pointed out that a calibration of inventory concentration or EIC is of minor relevance if one is interested in obtaining total fluence rates or dose rates at ground level. Here ESC or ESD are better quantities.

3.7 Common problems

During field measurements one cannot in general assume that the depth distribution of activity or the *equivalent depth of deposition* is the same everywhere. The errors introduced in this way influence the results in the same way irrespective the method of interpretation – ESC, ESD, or proposed EU. If an area A has a deeper deposition of radioactivity than another area B then the "signal" (e.g. the window net count rate) for area A could for example be 12% lower than for area B. Then all methods for interpretation will produce a concentration for area A that is 12% lower than for area B.

The same holds for the influence of a non-isotropic detector as for example a 10cm x 10cm x 40cm CGS detector. When this detector is used in an area inhomogeneously contaminated it will produce results that depend on its position and direction. This deviation from a "true mean value" will influence all methods of interpretation by the same amount. This is easily seen by recognising that it is the detector (window) count rates that are used for interpretations – and the count rate is of course independent of how one is going to interpret the results.

3.8 Calibration recommendations for mobile gamma spectrometry systems

Definitions:

ESD, equivalent surface deposition, is the activity per unit area deposited on an infinite, plane surface that will produce the same primary photon fluence rate at a certain energy one meter above the surface as the actual depth distributed source. The angular distribution of the

primary photon fluence from the equivalent surface deposition and the actual source can be different.

ESC, equivalent surface concentration, is that amount of true, homogeneous surface contamination per unit area that gives the same primary photon fluence rate at a certain energy at a specified height above the ground as does the actual depth distributed source.

EIC, equivalent inventory concentration, is the amount of true activity deposited per unit area with a specific depth distribution that gives the same fluence rate at survey altitude as the actual distribution of activity.

All systems should have a base calibration for measuring either ESD or ESC. All teams should be able to convert their base calibrations to EIC if a depth distribution is specified. The adjustment of the calibration should be based on tables or curves that have been generated beforehand. For conversion to EIC there should be numbers produced for different heights above ground level, e.g. 1.0 m, 1.5 m, 2.0 m, 2.5 m, 60 m, 80 m, 100 m and 120 m, and curves or formulae should be available. As a first approximation those numbers/curves could simply be based on conversion ratios for fluence rates, i.e. they are common for all systems. Later minor adjustments could be included for the angular dependence for those detector systems (plus platforms) that have a significant angular dependency.

In an emergency situation, if some systems have an unsatisfactory base calibration, an actual ESD calibration could be used. This should be done by selecting a calibration area of suitable size and with a depth distribution assumed typical for the area to be investigated. Systems already having a reliable calibration for measuring ESC or ESD with a known depth distribution could use a preliminary depth distribution for the area to be investigated. This preliminary depth distribution should later be replaced by a final depth distribution.

3.9 Relations between ESC, exponential depth distribution and inventory concentration

It is often assumed that for some time after a fall-out of radioactivity the depth distribution of for example ^{137}Cs could be described by an exponential function (Ref. 12, 7 and 4), i.e.

$$q(z) = q_0 \cdot \exp(-\alpha z) \quad (19a)$$

or

$$q(z) = q_0 \cdot \exp((-\alpha/\rho)(\rho z)) \quad (19b)$$

Here $q(z)$ is the activity concentration (Bq/cm^3) at the depth z, and q_0 is the concentration at the surface (also in Bq/cm^3); α is the exponential activity distributions coefficient, ρ is the density and α/ρ is the exponential mass activity distributions coefficient. $\beta = \rho/\alpha$ is termed the relaxation mass thickness or relaxation mass per unit area (Ref. 12 and Ref. 4).

For a constant ρ, $\rho \cdot z = \zeta$ is termed the mass depth. Equation (19b) then can be rewritten to

$$q(z) = q_0 \cdot \exp((-\alpha/\rho)\zeta) = q_0 \cdot \exp(-\zeta/\beta) \quad (20)$$

(A general definition of mass depth ζ also for non-constant density $\rho(z)$ can be found in Appendix A).

The activity (per unit area) within the depth interval from z to z + Δz becomes $q(z) \cdot \Delta z = q_0 \cdot \exp(-\alpha z) \cdot \Delta z$; and the inventory concentration Q (Bq/cm^2) becomes

$$Q = \int q(z) \cdot dz = \int q_0 \cdot \exp(-\alpha z) \cdot dz = q_0/\alpha \quad (21)$$

The relaxation mass thickness $\beta = \rho/\alpha$ was defined above for a distribution where ρ and α vary proportional to each other, i.e. $\beta = \rho(z)/\alpha(z)$ is constant.

By using the relation $\zeta = \int^Z \rho(u) \cdot du$ one has $d\zeta = \rho(z) \cdot dz$ or $dz = d\zeta/\rho(z) = d\zeta/\rho(\zeta)$. Therefore Equation (21) can be written

$$Q = \int q_0 \cdot \exp(-(\alpha/\rho) \cdot \rho z) \cdot dz = \int (q_0/\rho(\zeta)) \cdot \exp(-\zeta/\beta) \cdot d\zeta \quad (22)$$

If $\rho(\zeta)$ is a constant, then $\alpha(\zeta)$ also becomes a constant and the integration gives

$$Q = \int (q_0/\rho) \cdot \exp(-\zeta/\beta) \cdot d\zeta = \int (q_0 \cdot \beta/\rho) \cdot \exp(-\zeta/\beta) \cdot d\zeta/\beta = q_0 \cdot \beta/\rho = q_0/\alpha \quad (23)$$

The expression $(q_0/\rho(\zeta)) \cdot \exp(-\zeta/\beta) \cdot d\zeta$ is the activity found between the mass depths ζ and ζ + dζ.

From Equation (2) one gets the fluence rate $\varphi(h_A)$ at the height h_A in the air

$$\varphi(h_A) = \Sigma \Delta\varphi(h_A, z_G) = \Sigma \Delta q_G(z_G) \cdot E_1(h_A \cdot \mu_A + z_G \cdot \mu_G)/2 \quad (24)$$

$$\varphi(h_A) = \Sigma q_0 \cdot \exp(-\alpha z_G) \cdot \Delta z_G \cdot E_1(h_A \cdot \mu_A + z_G \cdot \mu_G)/2 \quad (25)$$

Here the summation should include all depths z_G with activity. Transforming to mass depths one has

$$\varphi(h_A) = \Sigma (q_0/\rho(\zeta)) \cdot \exp(-\zeta/\beta) \cdot \Delta\zeta \cdot E_1(h_A \cdot \mu_A + \zeta \cdot (\mu/\rho)_G)/2 \quad (26)$$

The ESC is found from demanding that the same fluence rate should be generated by a surface deposition with concentration equal to ESC.

$$\varphi(h_A) = ESC \cdot E_1(\mu_A \cdot h_A)/2$$

$$ESC = [\int (q_0/\rho(\zeta)) \cdot \exp(-\zeta/\beta) \cdot E_1(h_A \cdot \mu_A + \zeta \cdot (\mu/\rho)_G)\, d\zeta\,] / E_1(\mu_A \cdot h_A) \quad (27)$$

4 DEPTH DISTRIBUTION AT THE REFERENCE SITES

It has been discussed in Section 3 how the term equivalent surface concentration should be defined. Also it was discussed whether ESC is a sensible quantity or not for information of contaminant levels. When the depth distribution of the surveyed area is not known the calculation of ESC or ESD is one way to obtain information of the activity level. However, if the depth distribution is known it is possible to plot the inventory concentration, i.e. the real amount of radioactivity in the ground. To determine a depth distribution properly one has to take a lot of soil samples from within the measured area. Analysis of these takes a long time. If in some way information on depth distribution could be derived directly from the measured spectra a lot of time could be saved – both in the laboratory and in the field. This section deals with an attempt to derive information on depth distributions from the spectra measured at RESUME99. The measured spectra are compared with mean mass depths calculated from soil samples taken in connection with the RESUME99 exercise.

4.1 Mean mass depth at the reference sites

In order to examine spectrum shapes at the reference sites (measured with CGS systems) for "depth" signals it was necessary to have estimates of the mean mass depth for the sites. In connection with the Gävle exercise several soil core samples from those reference sites were examined in order to calculate the total inventories and depth profiles (Ref. 13). The core samples were sliced and the concentration of ^{137}Cs was determined for each layer. The data from the soil sampling also include densities for the individual layers which makes it possible to calculate a mean mass depth for ^{137}Cs. (Wet densities were used in the calculations.)

A special mean mass depth, $\zeta_{M,E}$ (g/cm^2), was calculated for three of the four reference sites: Harnäs, Regementsparken (Gävle) and Älvkarleö. No core sampling results from Utvalsnäs were available. The reference site at Utvalsnäs also differs from the other sites. At Utvalsnäs the car was parked at a roadside whereas the other three sites were lawns or natural ground.

Calculations were done for three different altitudes:
1.0 m, corresponding to *in-situ* measurements
2.2 m, corresponding the CGS measurements
100.0 m, corresponding to AGS measurements (equivalent altitude including aircraft body).

The mean mass depths were calculated according to Equation (8):

$$ESC \cdot \zeta_{M,E} = \Sigma \, [ESC(h_A,h_G) \cdot \Sigma \, \Delta h_G \cdot \rho_G(h_G)] \qquad (8)$$

In short, the equivalent mean mass depths $\zeta_{M,E}$ were calculated from the equivalent surface concentration, ESC, which itself was calculated from the information on the activities in the layered samples. For each depth interval the ESC for unit activity was multiplied with the activity for the same depth interval to obtain the ESC for the individual depth interval. Next the ESC for each layer was multiplied with the (mean) mass depth for the each layer. The equivalent mean mass depth for the entire soil sample was then calculated as the sum of all products divided by the sum of all ESC´s.

The ESC for unit activity as a function of accumulated mass depth was found from curves describing the ESC per unit activity as a function of mass depth and height above the ground. The calculation of the curves that are based on a horizontally homogenous distribution of

activity is also described in Section 3, Figure 3.1 and Figure 3.2. Table 4.1 shows the calculated equivalent mean mass depths for the three reference sites.

Table 4.1. Equivalent mean mass depths $\zeta_{M,E}$, ESC, and ESC ratios based on samples at three reference sites.

	Altitude m	ESC Bq/m2	Mean $\zeta_{M,E}$ g/cm2	AGS and *in-situ* ESC relative to CGS ESC
Regementsparken	1	16900	3.26	120 %
	2.2	20000	3.31	100 %
	100	39400	4.09	48 %
Harnäs	1	35900	2.44	118 %
	2.2	42100	2.47	100 %
	100	78100	2.97	52 %
Älvkarleö	1	10000	2.77	119 %
	2.2	12100	2.84	100 %
	100	24100	3.54	51 %

As expected, the calculated equivalent mean mass depths for the 100-m altitudes (AGS) are bigger then the other mean mass depths. The mean mass depths for 2.2 m (CGS) are bigger than the mean mass depths calculated for 1 m (*in-situ*) but not very much bigger. (The reason for AGS to "see" deeper into the ground is explained in Section 3.)

Table 4.1 also show ratios of CGS ESC relative to AGS and *in-situ* respectively. From calculations made on the core samples, on the average $ESC_{2.2m} \approx 1.19 * ESC_{1m}$ and $ESC_{2.2m} \approx 0.504 * ESC_{100m}$.

Table 4.2 shows the minimum and maximum equivalent mean mass depths derived from samples. Älvkarleö is by far the most homogeneous reference site judging from the small scatter interval.

Table 4.2. Minimum and maximum equivalent mean mass depths. Abbreviations in brackets are Core sampling numbers.

	Altitude m	Min. ζ g/cm2	Max. ζ g/cm2
Regementsparken	1	2.64 (G09)	3.49 (G07)
	2.2	2.66 (G09)	3.69 (G07)
	100	3.19 (G09)	4.61 (G07)
Harnäs	1	1.95 (H08)	2.92 (H07)
	2.2	1.98 (H08)	2.96 (H07)
	100	2.44 (H08)	3.61 (H07)
Älvkarleö	1	2.69 (A07)	2.90 (A09)
	2.2	2.73 (A07)	2.97 (A09)
	100	3.41 (A07)	3.72 (A09)

Figure 4.1 shows a graphic display of the intervals. All scatter intervals for each height overlap.

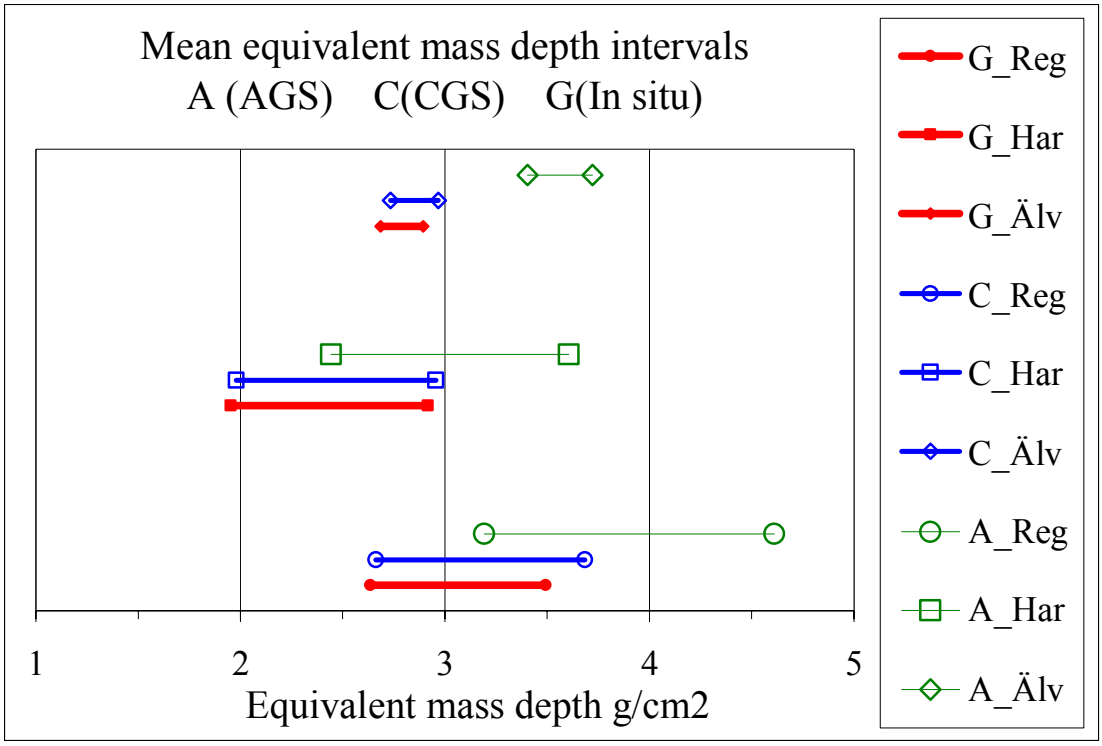

Figure 4.1. Equivalent mean mass depths – intervals.

4.2 Spectral shapes at selected distances along the definitive route

One of the aims of the data processing was to investigate the possibilities of extracting information on depth of burial of ^{137}Cs from the spectral shapes.

In order to compare the spectral shapes related to ^{137}Cs only one has to remove all information in the measured spectra related to the natural radionuclides thorium, uranium, and potassium. This turned out to be a tedious task. In Ref.14 the spectral shapes of mean spectra for four different road distances were compared. Figure 4.2 shows the mean spectra.

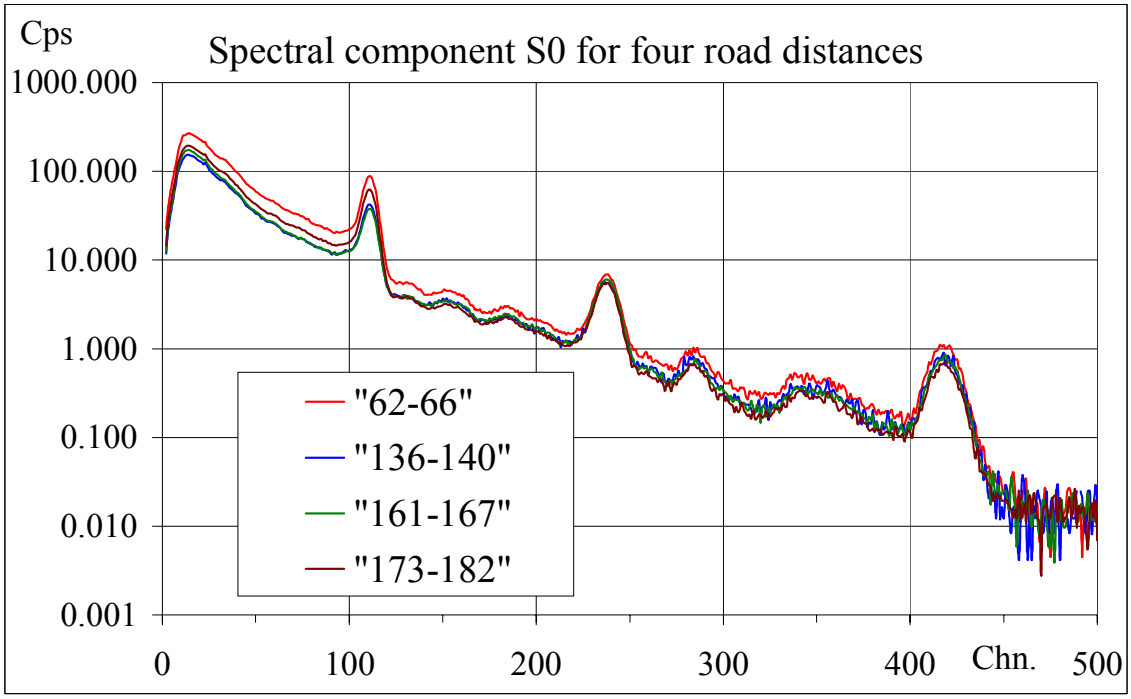

Figure 4.2. Mean spectra for distances along the definitive route.

First the spectra were compared by scaling the height of the ^{137}Cs full energy peak in the hope that the contribution from the natural radionuclides would show to be of little influence due to the high caesium contents. This did not give good results.

Next, the contribution from natural radionuclides was removed by subtracting (almost) pure spectra of Th, U, and K from measurements made on the calibration pads at Borlänge. Still it was not possible to get a reliable result. The limited size of the calibration pads meant that a portion of the scattered radiation at the low energies was missing – and because this was a spectrum region of great interest it was feared that whatever information could be found in the original spectra would be destroyed when subtracting Borlänge spectra.

It was then tried to subtract a measured spectrum (mean of three spectra) with a content of natural radionuclides close to that of the four mean spectra (approximately same U/Th and U/K ratios). Because of poor counting statistics this gave a distorted look to the resulting spectra. Also slight spectrum displacements (spectrum drift during measurements) made it difficult to remove all contribution from the natural radionuclides.

Furthermore, it was examined whether NASVD-processing (Ref.15, Ref. 16, Ref. 17 and Appendix B) of the data could produce a specific spectrum shape related to depth distribution. Such spectrum shapes were found. Spectral component number two, S2, in many cases comprised a caesium full energy peak and a “scattered radiation region” in anti-phase, see Figure 4.3.

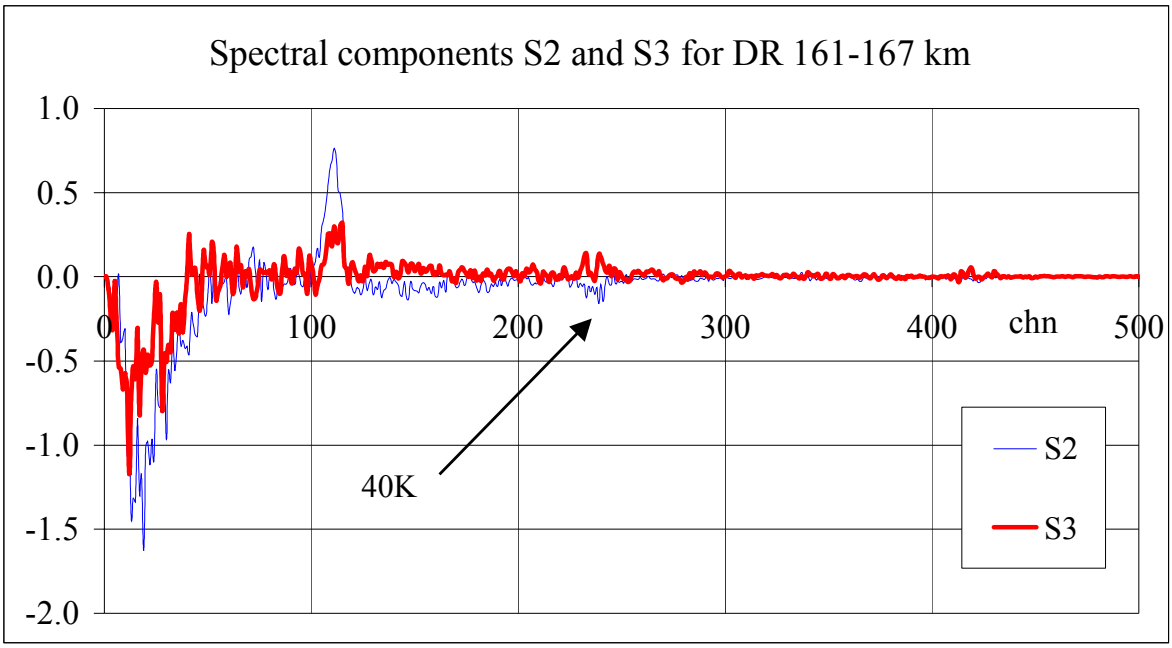

Figure 4.3. Spectral component S2 and S3 for the distance 161-167 km along the definitive route.

Unfortunately, this spectral component also contained information on (mostly) potassium. Sometimes more than one "depth" component would turn up as is the case in Figure 4.3. Spectral component S2 and S3 contain both scattered radiation and caesium full energy peak in anti-phase. The difference between S2 and S3 is caused by anti-phase potassium peaks. S2 + S3 "eliminates" the net K signal in the K-window. It was not possible to eliminate the potassium and thorium contributions from S2 by adjusting with the other spectral components.

4.3 Spectral shapes at the reference sites

After calculation of the mean mass depth (Section 3.4) it was decided to compare the depths with the spectral shapes of Danish CGS-spectra from the reference sites.

The reference spectra were NASVD-processed together. Next the spectra were reconstructed. (The measurements at the reference sites were performed with the car parked. Most NASVD spectral components should therefore contain only noise that can be removed.) The results showed, however, a strong spectrum drift in spectral component S3, Figure 4.4.

The Harnäs reference site was identified as the problem. The amplitudes b2 and b3 (not shown) both have two "levels". Amplitude b1 and b2 are shown in Figure 4.4. It is the deviation from the mean value for all sites that is shown in the figure. b1 represents the "concentration" of ^{137}Cs.

The last 40% of the Harnäs measurements were removed from the file and the NASVD processing was repeated. Still spectral component S2 and S3 contained noise (not shown) but the extra level seen for Harnäs had disappeared.

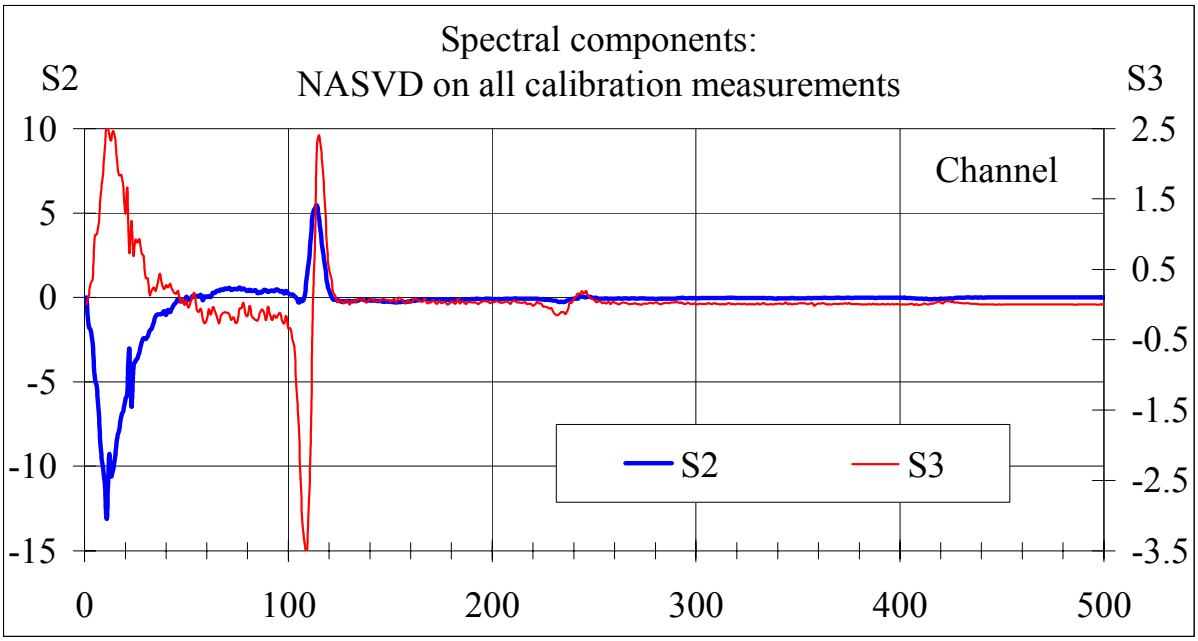

Figure 4.4. Spectral component S2 and S3 from NASVD on all calibration measurements.

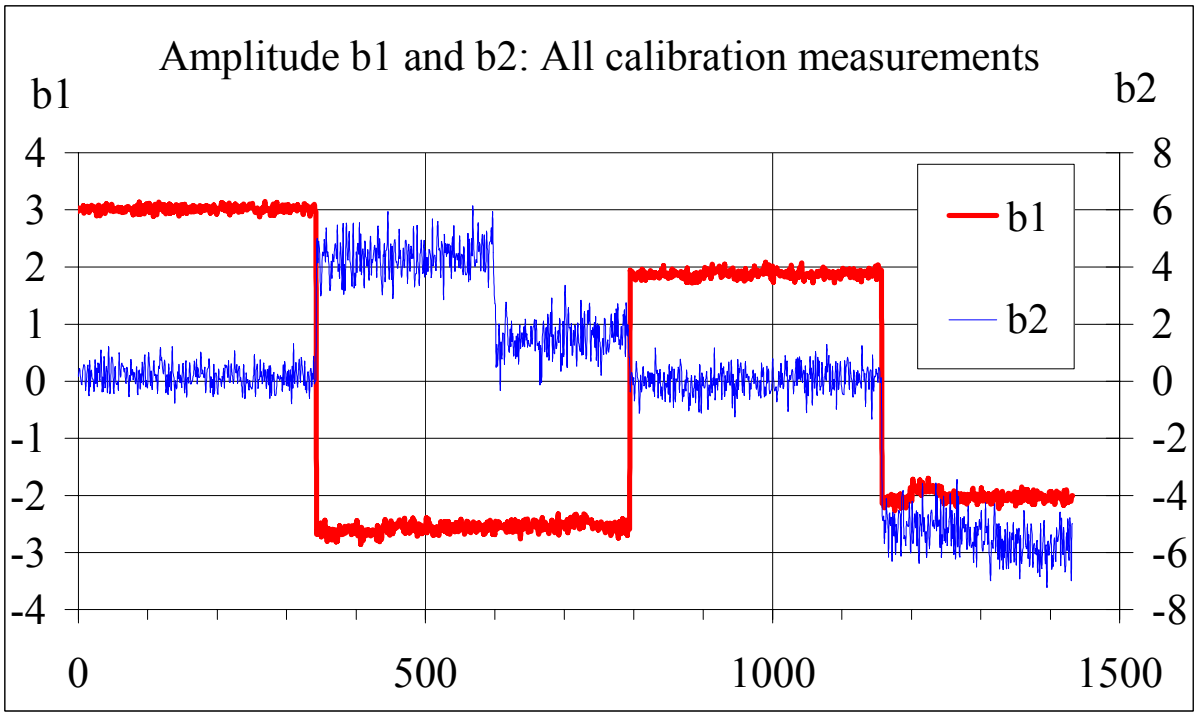

Figure 4.5. Amounts of spectral component S1 and S2 contained in the measurements. NASVD procession of all reference measurements. Plateaux from left to right (b1): Älvkarleö, Harnäs, Regementsparken and Utvalsnäs.

The reference spectra were reconstructed and are shown in Figure 4.6. The spectrum from Utvalnäs looks different than the others. The ratio of Th/K is high compared with that of the other three spectra.

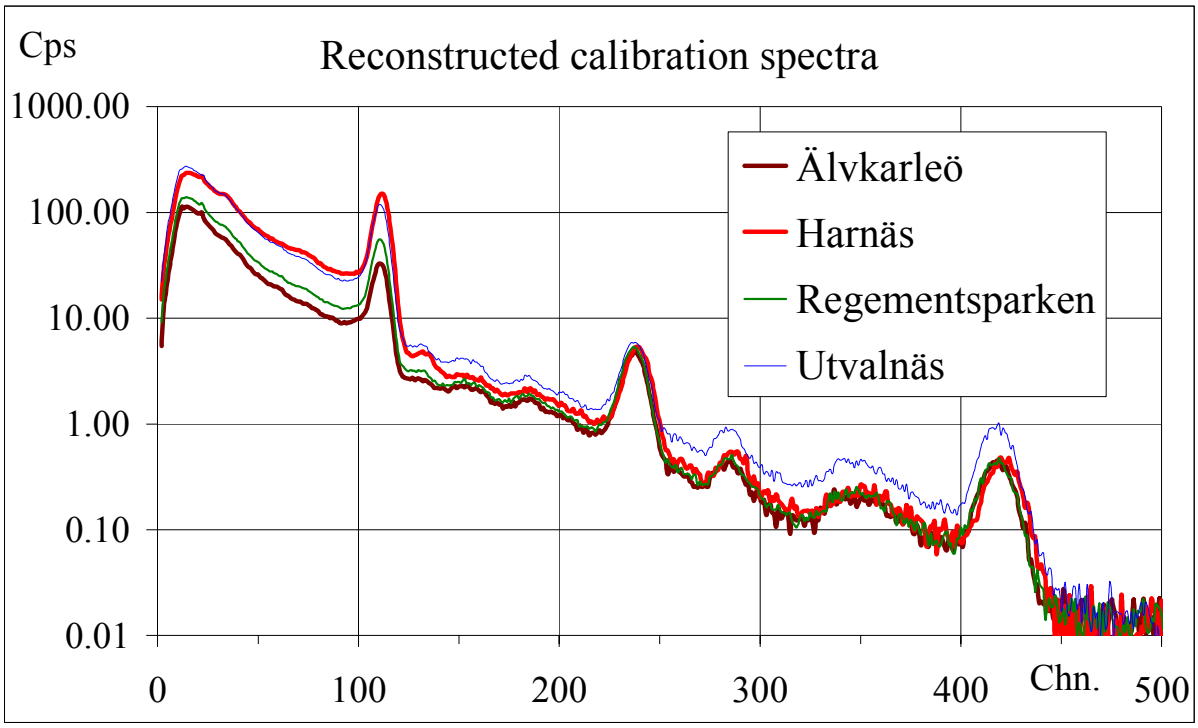

Figure 4.6. Mean spectra from the reference (calibration) sites, stationary measurements.

In order to remove the contribution from thorium, uranium and potassium to the spectral shapes at least two spectra containing different amounts of the natural radioisotope signals had to be used. These two "real" spectra were found from combinations of the earlier mentioned spectra from four distances along the definitive route. The four distances along the definite route used can be seen in Table 4.3.

Table 4.3. Information on mean spectra along the definitive route.

Distance km	Road type		Whereabouts
62-66	Gravel	Road, type 2	After Hästmuran to Bönan
136-140	Asphalt	Road, type 8	Östanbyn to Högtorp
161-167	Gravel	Road, type 8	Jordåsen to Åsberga
173-182	Gravel	Road, type 8	After Glamsen to Dalen

By subtracting the spectra from one of the others three almost "caesium-free" spectra were made. Two of these, with different Th/K ratios were chosen, Figure 4.7.

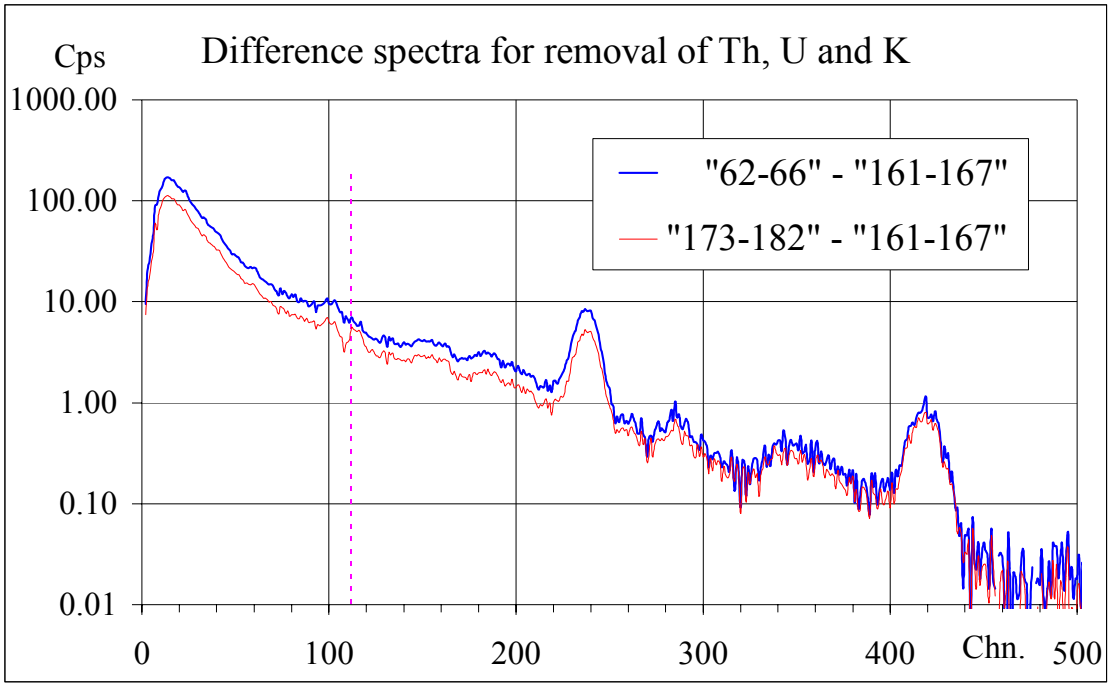

Figure 4.7. Spectra containing almost only natural radionuclides.

Spectrum "173-182" – "161-167" still seems to contain a little ^{137}Cs (dotted line shows peak centroid position). In the channels just before the possible caesium peak there is a small peak downwards. This is due to a slight difference in ^{214}Bi content. Figure 4.8 shows the spectra from the reference areas after subtraction of the (almost) caesium-free spectra and after scaling the spectra to fit the ^{137}Cs full-energy peaks.

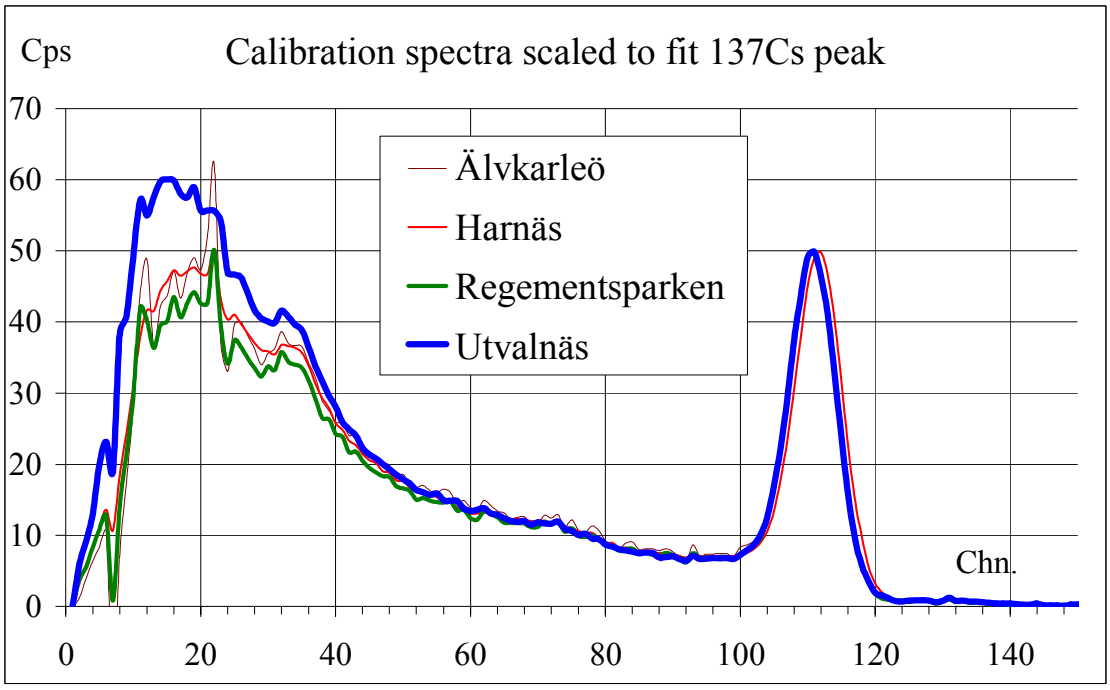

Figure 4.8. Reference spectra after attempt to remove natural radionuclides. The spectra have been scaled to match at the ^{137}Cs full energy peaks.

The spectrum from Utvalsnäs shows a larger signal at low energies compared to the other three spectra. The slight spectrum displacements observed earlier combined with a small change in ^{214}Bi level (change in amount of radon daughters?) have made some distortions at the lower energies. However, on the whole the resulting spectra are not very different from each other. The equivalent mean mass depth for Regementsparken (3.3 g/cm^2) was found to be slightly higher than for Älvkarleö (2.8 g/cm^2) that again was slightly higher than for Harnäs (2.4 g/cm^2). No information of mass depths for Utvalsnäs is available.

The calculated equivalent mean mass depths do not match with the spectral shapes calculated for the DKA1 CGS measurements. Here Älvkarleö > Harnäs > Regementsparken. It was expected that Regementsparken would show more scatterings at low energies than is the case. It should, however, be remembered that the uncertainty intervals for all reference sites do overlap. In reality the mean mass depth for all three reference sites may be the same. Only the spectrum from Utvalsnäs is significant different from the rest.

At the Technical University of Denmark laboratory simulations of different flight altitudes have been performed with the Danish AGS system B (Ref. 18). The different flight altitudes were simulated by using chip boards as attenuating material between source and detector. Each chip board is approximately 16 mm thick and has an average density of 0.74 g/cm^3. One chip board (i.e. approximately 10 m of air equivalent) corresponds to a mass depth of 1.19 g/cm^2.

Figure 4.9 shows two AGS spectra: 78.0 m and 87.75 m. The 78-m spectrum has been scaled for the two ^{137}Cs full energy peaks to be of the same size. The difference in scattered photons at the low energies represents the influence from a mass depth of 1.19 g/cm^2 for an airborne system. For a CGS spectrum the difference in mass depth would be smaller than 1 g/cm^2. The heights of the caesium peaks are approximately 50 cps for all spectra in Figure 4.8 and Figure 4.9.

Using Figure 4.9 for a primitive evaluation of the differences to be expected for the CGS spectra for Älvkarleö, Harnäs and Regementsparken one has to conclude that only minor differences between the spectra would be expected, and the sample results scatter so much that it is doubtful that the mean values based on samples really represent true mean values for the whole area. When also taking the uncertainties of the measurements into account one has to conclude that it has not yet been possible to correlate quantitatively the equivalent mean mass depth with the spectrum shapes for the measurements in RESUME 99.

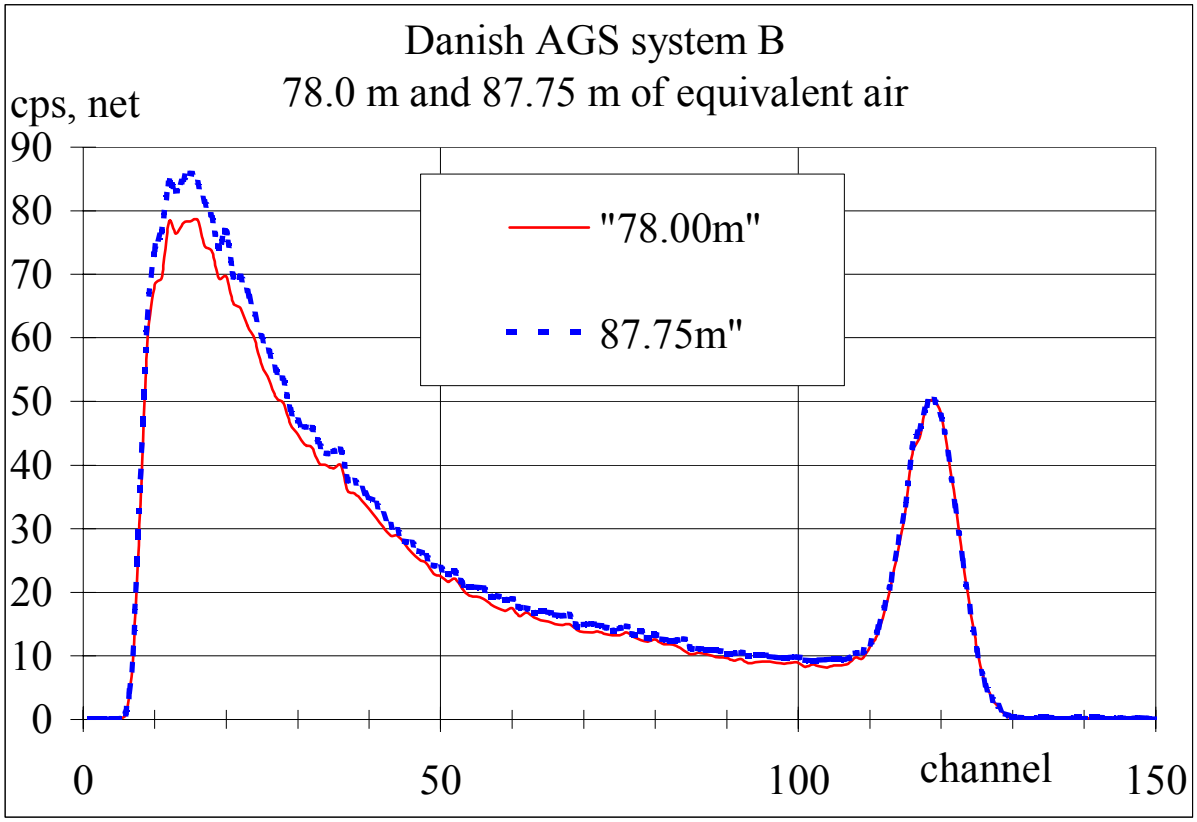

Figure 4.9. Airborne spectra measured in laboratory calibration set-up with Danish system B. The spectra corresponds to flight altitudes 78.0 m and 87.75 m respectively, i.e. a mass thickness difference of 1.199 g/cm^3. Measurements performed by M. Haase, January 1999 (Ref. 18).

5 CGS-AGS INTEGRATION

5.1 Data material

A large database has been collected to use for research within the NKS BOK-1.2 project. During the exercise RESUME 99 there were eleven CGS systems used to measure ^{137}Cs along the 200 km calibration route. The systems were carried by nine different cars. The sizes of the NaI(Tl) crystals varied between 3" x 3" (0,3 litres) and 4 litres and the integration time for each measurement varied between two and ten seconds. In May 2000 the Geological Survey of Norway (NGU) performed measurements along the calibration route with a CGS system containing a 16 litres crystal and with an integration time of only one second. To facilitate a detailed comparison, all the data have been processed and fitted to a fixed route with intervals of ten meters, which in the project was called the definitive route, DR. Since the systems were of many different types and the calibrations varied between the different teams it was decided to normalise all data. The system DKA1 was chosen to be the reference. A data set for a "median car" was also produced for use in the research on CGS-AGS integration. NGU performed the processing of the car-borne data (Appendix C and Ref. 20).

The RESUME 99 exercise did not include airborne measurements of gamma radiation but was concentrated on *in-situ* and car-borne measurements. However, The Swedish Gelogical Survey (SGU) had mapped the area based on airborne surveys in 1997 and 1998. The measurements were performed at a flying altitude of 60 metres with a line spacing of 200 metres. The sampling rate was 4 Hz, implying a sampling distance of 16 m along the flight lines. In order to compare car-borne and airborne results it was necessary to interpolate amongst the AGS data to relate those to the DR. This was carried out by the Swedish Radiation Protection Authority (SSI), (Ref.19).

Apart from measurement data there were also several types of descriptive data appended to the DR, useful for a deeper understanding of the response of the measurement systems. Differences in response could be expected depending on road type and road width. Asphalt-road and gravel-road data were therefore separated and information from the Swedish National Land Survey was used to divide all roads along the DR into three different widths (< 5 metres, 5-7 metres, > 7 metres). A number of different categories for land-use along the roads was also encoded to see whether response differences could be seen between agricultural areas, forest areas etc.

The data described above were all to a large extent used in the research within the project. The database also contains measurements from the second task in RESUME 99 when almost all roads in the Gävle area (50 x 50 km) were covered with CGS measurements. Additional data in the database are spectral information from all measurements, dose rate and nuclide specific measurements on four calibration points and fourteen *in-situ* points and information from a detailed soil sampling on three of the four calibration points. Processed data on K, U, and Th also exist along the DR and from the mosaic measurement. All together it makes a very extensive and unique database.

5.2 AGS versus median car

To investigate possible differences in response of CGS systems depending on different road types and road widths a thorough investigation of the quotients between AGS and CGS measurements of ^{137}Cs was made by Simon Karlsson, SSI (Ref.21). The calculations were

made on normalised and smoothed data and both the AGS and CGS measurements were normalised to the DKA1 car.

Table 5.1. Quotients of normalised (to DKA1) ^{137}Cs results for AGS and CGS (median car) for different road types and road widths.

Road type/Road width	AGS/CGS (median car)	Number of records
Asphalt <5 m	1.01	1590
Asphalt 5-7m	1.11	6305
Asphalt >7 m	1.32	4187
Gravel <5 m	0.95	6836
Gravel 5-7 m	1.19	325

It was found that for asphalt roads the quotients AGS/CGS got slightly bigger as the roads got wider. This was also the case for the gravel roads, i.e. the ESC values for CGS systems seemingly got smaller on wider roads.

It was assumed that the quotients on gravel roads would be smaller since more ^{137}Cs can be expected on these roads than on asphalt roads. For roads <5 metres the quotient is indeed a little smaller while for roads 5-7 metres the effect is contrary. This indicates that ^{137}Cs content on gravel roads is much lower than expected, probably due to the fact that much of the activity has been washed away with rain fall or ploughed of the roads with snow. The remaining activity is in many cases buried under several layers of new gravel. Another factor that may affect these quotients is the geometry effect. For example there are generally more urban areas along asphalt roads, resulting in different measurement geometries for both AGS and CGS depending on road type.

Taking road types, road widths and different geometries into account the statistics are probably not good enough to take the calculated ratios for “true” values, i.e. to use the results in the future to relate AGS and CGS measurements to each other by multiplying with a constant. The question is also still open as to how the situation would have been for fresh fallout.

A detailed examination of the normalised AGS and CGS results revealed many places along the DR where the quotient deviated a lot from those values seen in Table 5.1. Mostly short sections where affected but sometimes several kilometres of the route had large differences between the AGS and CGS results. With the aim to explain these differences persons from SSI travelled the route once again in August 2000 and around fifty places or sections were picked out for detailed investigations (Ref. 22).

Figure 5.1 and Figure 5.2. Size and shape of the ditches and the content of ^{137}Cs in them explained many of the features seen.

It was seen that most of the differences could be explained by small-scale landscape changes resulting in strange measurement geometries for cars. Travelling over bridges, beside lakes or through road crosses with large surrounding asphalt surfaces often results in large variations between AGS and CGS. One factor that frequently resulted in large response differences for CGS was the size and shape of the ditches along the roads, and the content of ^{137}Cs in them. Many ditches had accumulated a lot of caesium after the Chernobyl accident. Dose rates were measured and sometimes exceeded by a factor of two dose rates in the surrounding terrain. It was also identified that some ditches probably had been dug after 1986 resulting in very low contents of ^{137}Cs here. A few local "hot spots" with very high ^{137}Cs-levels were also identified. From the investigation it was concluded that the effects from road type and road width is of minor importance compared to these other local variations.

Mainly the same conclusions were drawn from comparisons performed by DTU (Ref. 23). The Danish examination of the data included comparisons with information on land use, e.g. agricultural areas, forests, industrial estates and so on. There were indications of forests giving lower ratios, poor roads giving higher ratios and wide roads and by-passes giving low ratios.

As an example, Figure 5.3 and Figure 5.4 show the equivalent surface concentrations of ^{137}Cs for two CGS system together with ESD calculated by SGU for an airborne system, along the last 20 kilometres of the DR. The AGS concentrations had been multiplied by SGU with a factor of two to correct for decay and penetration into the ground since 1986. In the figures the AGS concentrations have been divided by 2, i.e. the actual measured values were used. Figure 5.3 shows the curve for the CGS system SEA1 and Figure 5.4 shows the curve for the CGS system DKA1. The data has not been normalised but interpolation to fill gaps between co-ordinates has been performed. Road types and land use are also shown in the figures.

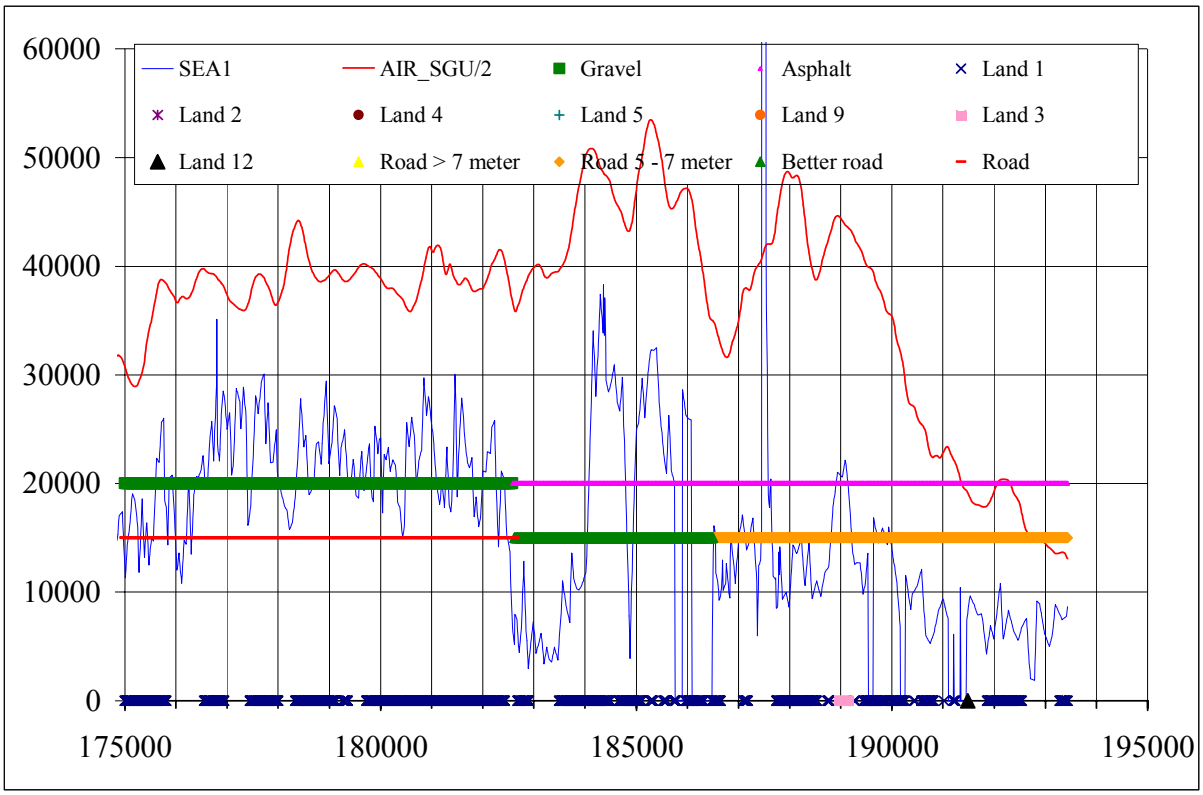

Figure 5.3. ESD for ^{137}Cs along the last part of the definitive route: CGS system SEA1 compared to the AGS measurements by SGU (divided by 2).

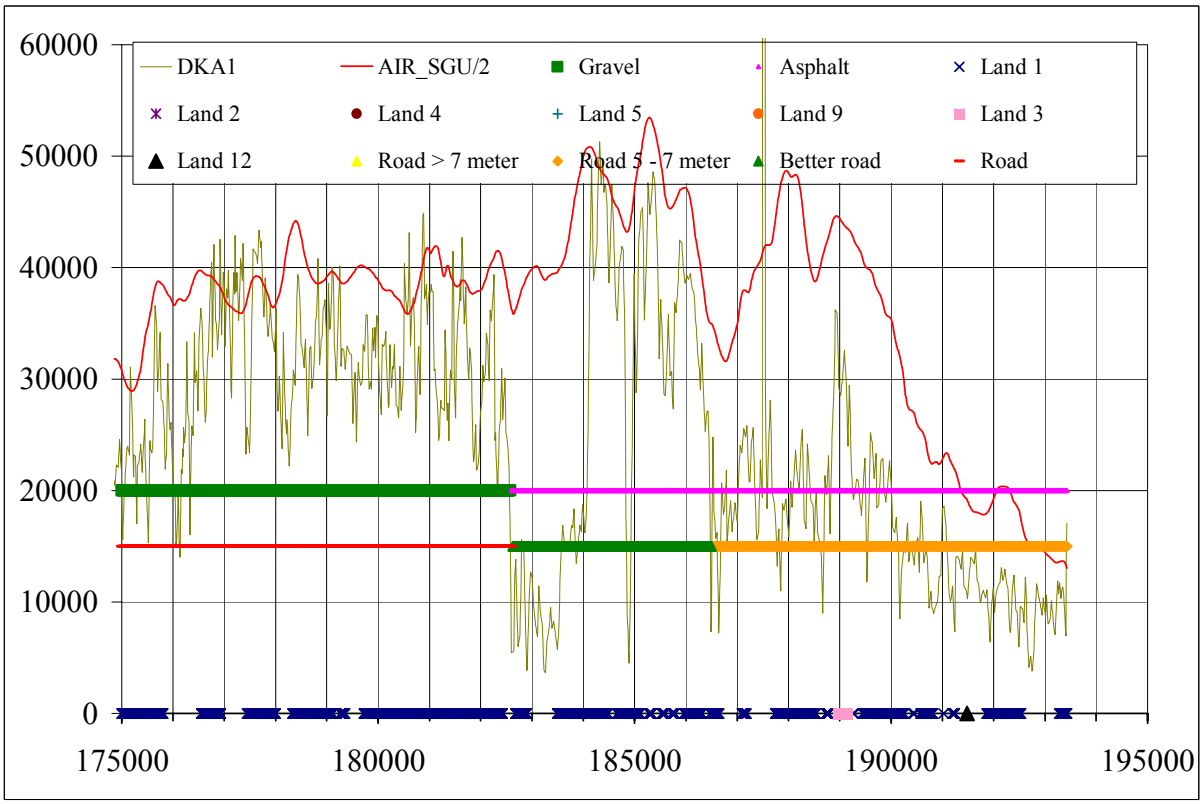

Figure 5.4. ESC for ^{137}Cs along the last part of the definitive route: CGS system DKA1 compared to the AGS measurements by SGU (divided by 2).

From the two figures it is clearly seen that the CGS curves fluctuate a lot more than the AGS curve. This is mainly due to frequent changes in the CGS measurement geometries. It is also seen that the ^{137}Cs-levels for the two cars and the AGS measurements are different. Car DKA1 shows around 40 % higher ^{137}Cs concentrations than SEA1. This is mainly due to different definitions of ESC and ESD. At the distances 177000-182000 and 184000-186000 the ESC for DKA1 is actually close to the AGS whereas this is not the case for SEA1. For the two Swedish systems (AGS and SEA1) the difference in general seems to be around a factor 2 (cf. Section 4.3). Because of these differences much of the research was made on normalised data.

Mostly the AGS and CGS curves show the same shape tendencies but there are several sections where large differences can be seen. These features can be found in both figures, i.e. both CGS detectors respond in the same way. Table 5.2 summarises the most obvious differences.

Table 5.2. Differences between AGS and CGS along the last 20 kilometres of the DR.

Distance (m)	**Explanation**
182360-184120	In this section the CGS response is drastically lowered while there is no change in the AGS level. According to SSI (Ref. 22) it was found from physical examination of the section that there was a distinct border in the ditches where ^{137}Cs levels changed to a higher level. This is probably due to the fact that part of the ditch has been re-dug after the Chernobyl accident. In general the ditches were wide and deep along this road.
184890	In this point there is a short but drastic drop in the CGS response. The small change in AGS response is probably due to the same reason. This is where the road goes on a bridge above the motorway E4.
187170	A very high increase in CGS response that extends far out of the diagram. The high CGS peaks are caused by a hidden ^{137}Cs source used in the RESUME 99 exercise only.
192750	At this point there is a local lowering of the CGS response. The road crosses a river from Storfjärden. The “water effect” is also seen by the AGS system at the distance from around 190000 and onwards where a large part of the AGS field of view is related to Storfjärden (Ref. 23).

Differences between AGS and CGS like in the examples above can be seen along the whole DR. Most of them are easily explained by different measurement geometries for the two different platforms. Especially small-scale landscape changes frequently result in response differences for CGS systems. Although large differences between AGS and CGS can be identified it should be pointed out that there are also a lot of similarities A future integration is indeed possible as long as calibrations are performed correctly. In the figure below results for the “median car” and the AGS system is plotted along the whole DR. Here the results are normalised to DKA1 results again since the calibrations were different.

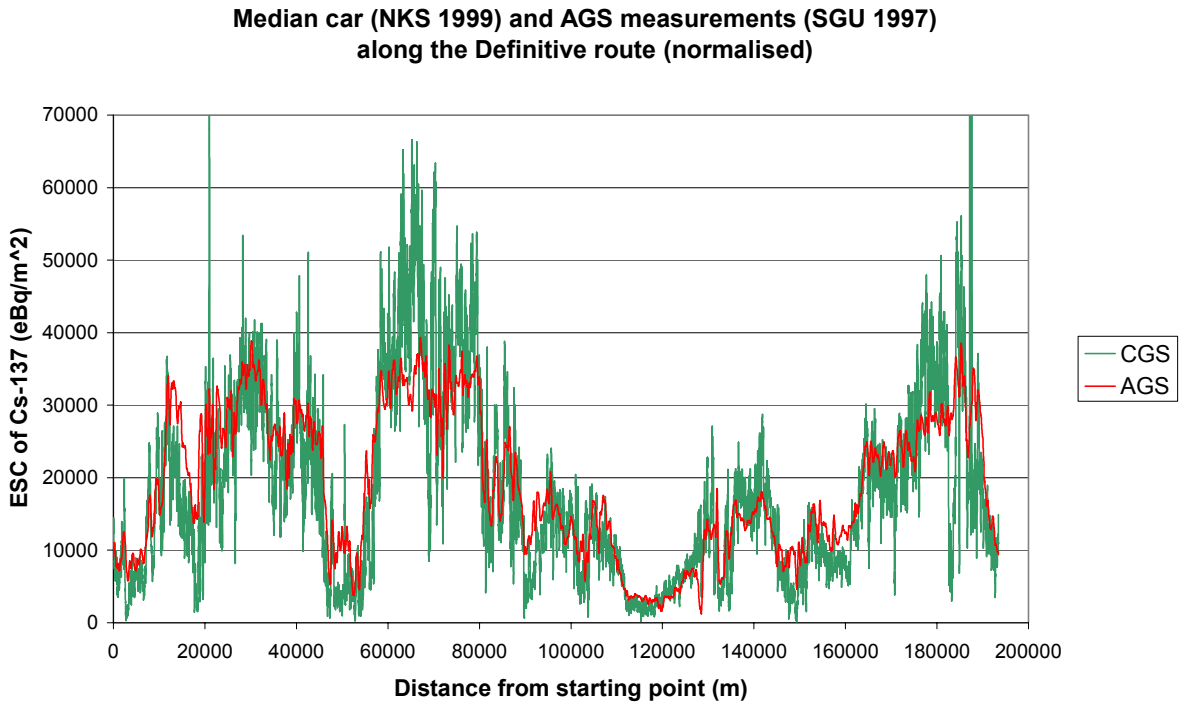

Figure 5.5. ESC for ^{137}Cs along the whole definitive route: AGS and CGS (median car) both normalised to system DKA1.

5.3 AGS versus car-borne system DKA1 and SEA1

From comparisons of the ESC results presented by the individual systems it was discovered that the results did not agree. It seemed that there were one group of car-borne systems showing approximately the same results and other groups of car-borne system presenting different results. It was at a later time (after the exercise) discovered from discussions amongst the NKS-members that the basic definition of ESC was inconsistent, cf. Section 3.

At DTU it was decided to make comparisons of AGS and CGS not using the median car results but using the results for the Danish DKA1 car only. Considering the fact that the AGS concentrations of ^{137}Cs calculated by SGU might be a result of a different ESC definition than that used for DKA1, the AGS concentrations used in the comparisons were concentrations previously calculated by DTU by a method called the "pseudo-concentration method" (Ref. 9, Appendix B). In these calculations the original Swedish data were used. Attenuation from aircraft and sensitivity had to be estimated from the values applying to the similar Danish AGS system.

Also, the AGS concentrations calculated by SGU were compared to the results for the Swedish car SEA1 assuming that the two systems were calibrated from the same definition of ESC. The Swedish AGS results originally produced for mapping had been multiplied with a factor 2 to take into account decay and penetration into the soil. In the comparisons with CGS this factor 2 was eliminated.

For examining the AGS/CGS relationship four distances, almost homogeneous with respect to land use, were chosen. Unfortunately it was only possible to find longer distances with homogeneous land use of forest. The chosen sections were also used in an attempt to relate

spectrum shapes to depth of burial for ^{137}Cs, see Section 3. One of the distances was an asphalt road and the others were gravel roads, Table 5.3.

Table 5.3. Information on mean spectra along the definitive route.

Distance (km)	Mean ESC* (kBq/m^2)	Road type	Whereabouts
62-66	42	Gravel road, type 2	After Hästmuran to Bönan
136-140	19	Asphalt road, type 8	Östanbyn to Högtorp
161-167	17	Gravel road, type 8	Jordåsen to Åsberga
173-182	30	Gravel road, type 8	After Glamsen to Dalen

*Calculated for the Danish system DKA1.

The ratios of ESC for CGS to AGS (based on measured spectra) are shown in Table 5.4 and Table 5.5. All results have been normalised to CGS ESC values of 100 kBq/m^2. DTU only has processed part of the data from the airborne survey of Gävle. The numbers in italics in Table 5.4 are estimated values only.

Table 5.4. Equivalent surface concentration and ratios for DKA1 CGS and AGS.

DR km	DKA1 CGS	AGS calculated by DTU method	CGS / AGS
62-66	100	193	0.52
136-140	100	189	0.53
161-167	100	*269*	*0.37*
173-182	100	*214*	*0.47*

Table 5.5. Equivalent surface concentration and ratios for SEA1 CGS and AGS.

DR km	SEA1 CGS	AGS calculated by SGU method, divided by 2	CGS / AGS
62-66	100	169	0.59
136-140	100	157	0.64
161-167	100	231	0.43
173-182	100	181	0.55

When compared with the ratios calculated for the layered soil samples in Section 4 it is seen that the CGS/AGS-ratios for the road measurements in general agree with those calculated theoretically from the samples for the reference areas with an exception for the distance DR 161-167 km. The calculation of ESC from core samples gave the relation $ESC_{2.2m} \approx 0.504\ ESC_{100m}$.

The calculated mean ESC for the distances 136-140 km and 161-167 km were rather similar. The first is an asphalt road and the second is a gravel road but both roads are of the same width. However, it cannot be concluded that the difference in ratios is caused by the one of the road being asphalt. The ratios calculated for the two other gravel distances are more in agreement with the result for the asphalt road than for the gravel road 161-167 km.

Comparisons AGS-CGS are not very reliable due to great influence from local phenomena on the CGS results. However, seemingly the ratio ESC_{CGS} / ESC_{AGS} calculated from rather homogeneous distances fits reasonably well with the ratio expected based on sampling at the reference sites.

The sensitivity distribution for CGS systems similar to DKA1, measured in Næstved, August 2000 (Ref. 8), shows that the area to the right of the car dominates the signals. It was also shown that the car attenuation downwards is effective. Therefore, the contamination of a road means less for a CGS system than for a free-in-air detector.

A transfer of fallout from the road to the roadside where it is easily detected by the CGS equipment has also taken place. The "disturbance" effect from the road is therefore limited and the ratio ½ found between ESC_{CGS} and ESC_{AGS} will therefore be approximately consistent with what one would expect from the test measurements at the reference sites and indicates that the depth distribution for the examined road distances is comparable to those observed at the reference sites.

6 ACRONYMS

AGS	Airborne Gamma Spectrometry
CGS	Car-borne Gamma Spectrometry
DEMA	Danish Emergency Management Agency
DKA1	DEMA car-borne spectrometry system
DTU	Technical University of Denmark
EIC	Equivalent Inventory Concentration
ESC	Equivalent Surface Concentration
ESD	Equivalent Surface Deposition
NASVD	Noise Adjusted Singular Value Decomposition
NGU	Geological Survey of Norway
SEA1	SSI car-borne spectrometry system
SGU	Geological Survey of Sweden
SSI	Swedish Radiation Protection Authority

7 REFERENCES

1. Byström, S. et al.: Airborne measurements with HPGe and NaI detectors in the Gävle area, Sweden. Field campaign 1997_1998, Geological Survey of Sweden (Uppsala, Sweden, 1998)
2. NKS-15, RESUME 99, Rapid Environmental Surveying Using Mobile Equipment, NKS, ISBN 87-7893-065-0, 2000
3. NKS-5, Planer for NKS-programmet 1998-2001, NKS, ISBN 87-7893-053-7, 1999
4. Sanderson, D. S. W., Allyson, J. D., Toivonen, H. and Honkamaa, T.: Gamma Ray Spectrometry Results from Core Samples Collected for Resume 95, in RESUME95, NKS, 1997. ISBN 87-7893-014-6.
5. Aage, H. K., Korsbech, U., Bargholz, K. and Hovgaard, J.: Gamma photon fluences above plane homogeneous area sources – and relations with Equivalent Surface Concentration. Report IT-NT-51, April 2000, IAU-DTU.
6. Korsbech, U., Bargholz, K. and Aage H. K. Problems with Integration of AGS and CGS. Differences and Similarities between Airborne and Carborne Gamma-Ray Spectromety. Report IT-NT-46, July 1999, IAU-DTU.
7. Finck. R.: Field Gamma Spectrometry and its Application to Problems in Environmental Radiology, cited in Calibration of carborne detectors for ESC of Cs-137 by Simon Karlsson, SSI, 10 January 2001.
8. Aage, H.K., Korsbech, U. and Bargholz, K.: Determination of Carborne Gammaray Spectrometry Sensitivities for ^{137}Cs (From Measurements with a Point Source.). Department of Automation, Technical University of Denmark. Report IT-NT-53, October 2000.
9. Aage, H.K., Bargholz, K. and Korsbech, U.: CGS and In Situ Measurements in Gävle 1999. RESUME99. (Draft edition.) Department of Automation, Technical University of Denmark. Report IT-NT-49, December 1999.
10. Bargholz, K.: Comparison of Airborne γ-Ray Detector Systems (French vs. Danish). Department of Electrophysics, Technical University of Denmark. Report NT-25 revised December 1996.
11. European Co-ordination of Environmental Airborne Gamma Ray Spectrometry. Status Report for Period January 1996 – December 1997. Annex V with Draft Standard Procedures for Deposition Mapping.
12. ICRU Report No. 53. Gamma-Ray Spectrometry in the Environment. ICRU, December 1994. ISBN-0-913394-52-1
13. Swedish Defence Research Establishment (FOA): Radionuclides in soil at the reference points. May-June 1999.
14. Comparison of CGS and AGS measurements of ^{137}Cs. RESUME99. NASVD construction of synthetic CGS spectra. Department of Automation, Technical University of Denmark, Restricted NKS-edition IT-NT-55, November 2000
15. Hovgaard, J. Airborne gamma-ray spectrometry. Statistical analysis of Airborne gamma-ray data. Ph.D. Thesis submitted to Department of Automation, Technical University of Denmark, October 1997.

16. Bargholz, K., Hovgaard, J. and Korsbech, U. Standard methods for processing data from the Danish AGS system. Department of Automation, Technical University of Denmark, IT-NT-36, April 1998.
17. Aage, H.K., Korsbech, U., Bargholz, K. and Hovgaard, J. A new technique for processing airborne gamma ray spectrometry data for mapping low-level contaminations. Applied Radiation and Isotopes 51/6, pp. 651-662, October 1999.
18. Haase, M. Standard and special gamma spectra for AGS equipment. Annual quality test of GR-820 γ-spectrometer system B. Department of Automation, Technical University of Denmark, Report IT-NT-41, January 1999.
19. Lindgren, Jonas: Description of the AGS data processing, Swedish Radiation Protection Institute, September 2000.
20. Smethurst, M.A.: Rapid environmental surveying using mobile gamma ray spectrometry: processing of results from the RESUME99 exercise, Gävle, Sweden. NGU Report 2000.087.
21. Karlsson, Simon: AGS/CGS quotient along the Definite Route, Swedish Radiation Protection Institute, September 2000.
22. Karlsson, Simon: Investigation of the definitive route, Swedish Radiation Protection Institute, September 2000.
23. Aage, H. K and Korsbech, U.: AGS and CGS response along the definitive route: Similarities and differences. Note, Department of Automation, Technical University of Denmark, Lyngby, September 2000.
24. Smethurst, M.A.: A mobile gamma ray spectrometer system for nuclear hazard mapping. NGU (2000) Report 2000.088.

APPENDIX A. Definitions

Activity per unit area
The activity per unit area, A_a, in Bq/m^2, is the activity contained in a vertical column of stated depth divided by the cross sectional area. Also see Inventory Concentration.

Concentration of radioactivity

q	Activity per area.	(Bq/cm^2)
q	Activity per mass or volume.	(Bq/g or Bq/cm^3)

Effective or equivalent mean mass depth
Effective or equivalent mean mass depth (g/cm^2) for ^{137}Cs is the mean mass depths for ^{137}Cs activity weighted by for example the ESC-values for the activity instead of being weighted by the activity itself.

Equivalent Surface Concentration – ESC
The Equivalent Surface Concentration (kBq/m^2) is that amount of true, homogeneous surface contamination per unit area that gives the same primary photon fluence rate at a certain energy at a specified height above the ground as does the actual depth distributed source. Mathematically the ESC is calculated as $ESC = \Sigma\, \Delta q_G(h_G) \cdot E_1(h_A \cdot \mu_A + \zeta \cdot (\mu/\rho)_G) / E_1(h_A \cdot \mu_A)$

Equivalent Surface Deposition – ESD (or Equivalent Surface Activity)
The equivalent surface deposition is the activity per unit area deposited on an infinite, plane surface that will produce the same primary photon fluence rate at a certain energy one meter above the surface as the actual depth distributed source. The angular distribution of the primary photon fluence from the equivalent surface deposition and the actual source can be different.

Equivalent Inventory Concentration – EIC
The Equivalent Inventory Concentration (kBq/m^2) is the amount of true activity deposited per unit area with a specific depth distribution that gives the same fluence rate at survey altitude as the actual distribution of activity.

Inventory Concentration
Inventory Concentration (kBq/m^2) is the total amount of activity per unit area integrated to a specified depth. The depth could be 20 cm to 40 cm. The symbol Q is used for inventory concentration.

Mass depth ζ
Mass depth ζ (g/cm^2) corresponding to a depth z is the integrated mass per unit area down to z,

$\zeta = \int^z \rho(u) \cdot du.$

Relaxation mass thickness β
Relaxation mass thickness β, or relaxation mass per unit area, (g/cm^2) is the relaxation parameter for a concentration that decreases exponentially with mass depth.

$q(z) = q_0 \exp(-\zeta/\beta).$

APPENDIX B. Analysis techniques

NASVD

The Noise Adjusted Singular Value Decomposition (NASVD) technique could be considered an extension of the ordinary Singular Value Decomposition method. However, the amount of the statistical noise of the spectra has been taken into account in the decomposition.

Consider a data set with J NaI(Tl) spectra each including N channels with counts. NASVD extracts a set of spectral components - $\boldsymbol{s}_o$, $\boldsymbol{s}_1$, $\boldsymbol{s}_2$, etc. - also spectra with N channels. These spectral components contain all spectral information of the whole set of data. By linear combinations of the spectral components all measured spectra can be reconstructed.

Reconstruction: $$\boldsymbol{r}_j = \boldsymbol{s}_o + (\boldsymbol{s}_1 b_{j1} + \boldsymbol{s}_2 b_{j2} + ... + \boldsymbol{s}_{max} b_{jmax})/LT_j \quad (28)$$

where $\boldsymbol{r}_j$ is the reconstructed spectrum number j. It is considered a vector with elements (channel count rates) $r_{j,n}$ with units of counts per second. b_{ji} is the amplitude (amount) of $\boldsymbol{s}_i$ to be included in the reconstruction of measured spectrum number j. $\boldsymbol{s}_i$ is also considered a vector. The unit of $\boldsymbol{s}_i$ is counts, except for $\boldsymbol{s}_o$ that has the unit counts per second. LT_j is the live time for measurement number j. Spectral component number zero - $\boldsymbol{s}_o$ - is equivalent to the *average of all spectra* in the set of data.

In principle there are as many spectral components as there are channels, i.e. N. To avoid most of the statistical noise one in general only uses spectral component number zero together with the next 4 to 9 components when reconstructing spectra. In an ideal situation one should only observe real signals in a number of spectral components equal to the number of independent gamma emitters. However, any factor that influences the spectrum shape may cause an additional spectral component (spectrum drift, altitude variations, variations in depth of burial, etc).

Spectral components of low numbers are more important than those of higher numbers. The average spectrum, $\boldsymbol{s}_o$, is the most important component, $\boldsymbol{s}_1$ is the second most important, etc.

The reconstructed spectra $\boldsymbol{r}_j$ can be processed by standard methods, e.g. the three-windows method commonly used for determination of the concentrations of Th, U, and K from CGS and AGS data.

The pseudo concentration method

The concentrations of ^{137}Cs can be calculated by the pseudo concentration method developed for NASVD processed data (Ref. 13). This technique was used by DTU on the AGS SGU data.

The pseudo concentrations are calculated from four synthetic spectra ($\mathbf{v_i}$): one synthetic caesium spectrum and three linearly independent spectra containing no ^{137}Cs but only mixtures of thorium, uranium and potassium and converted into physical concentrations by a conversion factor.

$\mathbf{v}_1 = a_{11}\mathbf{s}_1 + a_{12}\mathbf{s}_2 + a_{13}\mathbf{s}_3 + a_{14}\mathbf{s}_4$ synthetic Cs spectrum
$\mathbf{v}_2 = a_{21}\mathbf{s}_1 + a_{22}\mathbf{s}_2 + a_{13}\mathbf{s}_3 + a_{24}\mathbf{s}_4$ synthetic spectrum without Cs
$\mathbf{v}_3 = a_{31}\mathbf{s}_1 + a_{32}\mathbf{s}_2 + a_{33}\mathbf{s}_3 + a_{34}\mathbf{s}_4$ synthetic spectrum without Cs
$\mathbf{v}_4 = a_{41}\mathbf{s}_1 + a_{42}\mathbf{s}_2 + a_{43}\mathbf{s}_3 + a_{44}\mathbf{s}_4$ synthetic spectrum without Cs (29)

The "a" values for the synthetic caesium spectrum are selected to satisfy the following equations for $a_1 = -1$ (or a = 1).

$u_1 = a_1 f_{1,Th} + a_2 f_{2,Th} + a_3 f_{3,Th} + a_4 f_{4,Th} = 0$
$u_2 = a_1 f_{1,U} + a_2 f_{2,U} + a_3 f_{3,U} + a_4 f_{4,U} = 0$
$u_3 = a_1 f_{1,K} + a_2 f_{2,K} + a_3 f_{3,K} + a_4 f_{4,K} = 0$ (29a)

where $f_{i,x}$ is the window counts of the nuclide X window for spectral component No. i and u_i is the sum of the window counts of the nuclide X window. Equation (29) can be rewritten as a matrix equation

$$\mathbf{V} = \mathbf{AS} \quad \Rightarrow \quad \mathbf{A^{-1}V} = \mathbf{S} \quad \Rightarrow \quad \mathbf{DV} = \mathbf{S} \tag{30}$$

The matrix **D** is the inverse matrix to matrix **A**. The d_{i1} -value is the content of synthetic caesium spectrum $\mathbf{v}_1$ that is contained in spectral component i (this means, for example that $d_{1,1}$ is the content of caesium spectrum in spectral component s_1).

The physical caesium concentrations are calculated from the pseudo concentrations, h_i, and a conversion factor. The pseudo concentrations h_{j1} are calculated as

$$h_{j1} = h_0 + (b_{j1} * d_{11} + b_{j2} * d_{21} + b_{j3} * d_{31} + b_{j4} * d_{41})/LT_j \tag{31}$$

Since the mean spectrum including background is extracted from the NASVD-processed data file it is necessary to add to h_{j1} the amount of caesium contained in the mean spectrum (spectral component zero), h_0.

From measurements taken at flights over sea areas (background measurements) one is able to calculate h_0. (h_0 does not include caesium signals from the aeroplane.)

$$h_0 = -(b_{backgr,1} * d_{11} + b_{backgr,2} * d_{21} + b_{backgr,3} * d_{31} + b_{,backgr,4} * d_{41})/LT_{backgr} \tag{32}$$

For CGS measurements one may include background spectra measured with the car onboard a ship with a low content of ^{137}Cs. Pseudo concentrations are further discussed in Ref. 16.

Indirect method

The pseudo concentrations, h_j, are converted into ground level concentrations, c_j, in Bq/m^2

$c_j = G_H h_j$ G_H is a height dependent conversion factor (33)
$CR_{Cs,j} = s_H c_j$ s_H is the height dependent sensitivity (34)
and $CR_{Cs,j}$ is the caesium window net count rate
(both determined for a standard caesium window)

First the sensitivity for the equivalent flight altitude H, s_H, is calculated

$$s_H = s_{100}\, e^{-\mu,obs\,(H-100)} \qquad (35)$$

μ,obs is the attenuation coefficient and s_{100} the sensitivity of ^{137}Cs at 100 m equivalent altitude.

The mean background spectrum (NASVD processed background measurements) was subtracted from the mean spectrum for the data file. Both mean spectra are in the form of spectral component zero, $\boldsymbol{s}_o$, and includes the background. Thus the difference between the two $\boldsymbol{s}_o$ spectra will give the background corrected mean spectrum for the area.

The average net window count rate for ^{137}Cs, $CR_{Cs,aver}$ was determined from the difference spectrum. The average ground level concentration is then calculated as $c_{aver} = CR_{Cs,aver} / s_{H,aver}$.

The average pseudo concentration h_{aver} is calculated from Equation (31) and an average conversion factor, $G_{aver} = c_{aver} / h_{aver}$ is calculated as an estimate for G_H.

$$c_j \approx G_{aver}\, h_j \qquad (36)$$

Direct method

In the direct approach the calculations of h_0 and h_i are calculated in exactly the same way. The ground level concentrations, however, are calculated in a different way,

$$c_j \approx H h_j \qquad (36b)$$

$$H = C_{Cs,syn} / s_{H,aver}$$

In the direct method $C_{Cs,syn}$ is the count rate (peak net area) of the synthetic caesium spectrum. The synthetic spectrum is not influenced by background. (The background is included in spectral component $\boldsymbol{s}_o$, i.e. the mean spectrum. The synthetic spectrum does not include $\boldsymbol{s}_o$).

APPENDIX C. Post-exercise data processing

Data from mobile measuring teams participating in the RESUME-99 Fixed Route exercise were processed to facilitate a detailed comparison between the data sets. The fixed route was in the form of a 194 km closed loop passing through both rural and urban areas. Nine vehicles from 7 countries carried 13 separate measuring systems.

Results from the different measuring systems were projected into the known trace of the fixed route so that the results could be compared. Also, estimates of equivalent surface activity ^{137}Cs from the different car-borne measuring systems were normalised to data obtained by the Danish Emergency Management Agency (system DKA1) and combined to produce an overall (cross-system) ^{137}Cs profile for the fixed route. Furthermore, a ^{137}Cs profile for the fixed route was extracted from airborne gamma ray spectrometry data provided by the Geological Survey of Sweden (SGU), enabling a comparison between car-borne and airborne surveying methods. Original and processed data for the fixed route can be obtained from the NKS upon request. Ref. 24 offers a detailed account of the data processing and an index to the digital data sets.

The fixed route

All vehicles recorded their passage through the fixed route using the satellite-based Global Positioning System (GPS). Some of the vehicles were equipped to carry out real-time differential correction of the GPS data (DGPS). Navigational inaccuracies, gaps in navigational records due to temporary loss of GPS satellite coverage and other navigational errors led to significant differences between the recorded routes of the vehicles. These differences reach several hundred metres in places.

The Swedish Radiation Protection Institute (SSI) provided the actual co-ordinates of the fixed route into which the results from the various vehicles were to be projected. The route provided by the SSI comprised a series of irregularly spaced co-ordinates. To produce a more regular data set the route was re-sampled to generate co-ordinates at exactly 10 metre intervals along the road (19344 co-ordinates in all).

Projecting the car-borne data into the reference route

All measuring teams delivered data to the exercise organisers in the pre-determined NKS-format by the deadline of 22:00 on the day of the exercise. These data files were the starting point for the post-exercise processing described here. Minor editing was required to correct formatting errors in some of the data files. Short gaps in navigational records were interpolated over and then all measurements from the cars were projected or 'snapped' into the regularly spaced co-ordinates of the known route. The effect of the projection process on each data point is recorded in the processed data files in terms of distance projected and direction projected.

Elimination of unreliable and excess data

Where navigational errors and inaccuracies were large, projection into the fixed route was unreliable. Therefore, data that lay more than 100 m from the known route were rejected. Also, if more than one data item from any single measuring system projected into the same position in the known route, all but the first were rejected.

Merging data from all measuring systems into a single data table

The projection procedure and reduction of data to at most one measurement from each measuring system per position in the known route enabled the merging of data from all measuring systems into one processed data table with a single (common) co-ordinate set. The airborne gamma ray spectrometry data set of ^{137}Cs activities was sampled along the fixed route and the data inserted into the combined data table.

Normalising estimates of equivalent surface activity of ^{137}Cs and production of a single ^{137}Cs profile for the fixed route

Using the combined data table, all of the estimates of equivalent surface activity of ^{137}Cs made by car-borne measuring systems were normalised to the DKA1 system. The normalised ^{137}Cs data sets for the different measuring systems were reduced to a single overall result for the fixed route by selecting the *median* normalised car-borne measurement for each 10 m position along the route. If there were an even number of measurements for a particular position, the average of the two middle values was taken to be the median. If there were no measurements for a position in the route, a dummy value was assigned to that position.

To examine how alike the normalised results from the different measuring systems are, one can look at how often results from each measuring system were selected as median values in the production of the combined ^{137}Cs profile. The measuring systems with shortest integration time generally contributed more data to the median profile, simply because those systems produced more measurements during the exercise. If one examines the contributions of data to the median result after normalising the figures to sampling rate, the contributions from all the large NaI and HPGe systems become approximately equal and larger than the contributions from the smaller detectors, usually mounted lower and inside the vehicles. This is because the larger detector systems are in the majority, have similar high spatial resolutions and produce ^{137}Cs profiles with similar shapes after normalisation. The smaller detectors were fewer, had lower spatial resolutions and profile shapes were occasionally noisy.

Available data sets

Processing was carried out in stages at indicated above and the products of each processing stage are preserved in data files. This enables further manipulation of the data from any particular starting point in the processing sequence. Original and processed data sets for the fixed route exercise are available upon request from the NKS.

Title	Mobile Gamma Spectrometry. Evaluation of the Resume 99 Exercise
Author(s)	Hans Mellander,[1)] Helle Karina Aage,[2)] Simon Karlsson,[1)] Uffe Korsbech,[2)] Bent Lauritzen[3)] and Mark Smethurst[4)]
Affiliation(s)	1) Swedish Radiation Protection Authority, Stockholm, Sweden 2) Technical University of Denmark, Lyngby, Denmark 3) Risø National Laboratory, Roskilde, Denmark 4) Geological Survey of Norway, Trondheim, Norway
ISBN	87-7893-111-8
Date	June 2002
Project	NKS/BOK-1.2
No. of pages	51
No. of tables	10
No. of illustrations	16
No. of references	24
Abstract	During the RESUME 99 exercise, the radiocaesium (^{137}Cs) activity in the surroundings of Gävle in central Sweden was mapped using car-borne gamma-ray spectrometry (CGS). The CGS data along with airborne gamma-ray spectrometry (AGS) data from the same area have been used to examine possible correlations between the CGS and AGS results, detector type and position, and geographical information, such as land-use and road type. The overall differences between various CGS results are small, while larger differences are found between AGS and CGS results. In general only little correlation was found with land-use and with road-type and width. The differences between AGS and CGS results arise because airborne detectors have a different field of view than a ground-based detector. From an analysis of the depth-dependency of AGS and CGS data for a depth-distributed source, it is found that the mean mass depth may be inferred from the ratio of AGS to CGS spectral count rates. Integration of AGS and CGS data requires a precise definition of quantities and units for reporting activity concentrations in a complicated geometry and care must be taken to translate AGS results into equivalent CGS quantities taking into account the spatial distribution of the radionuclides.
Key words	Aerial Monitoring; Cesium 137; Comparative Evaluations; Gamma Spectroscopy; Radiation Monitoring; Vehicles

Available on request from the NKS Secretariat, P.O.Box 30, DK-4000 Roskilde, Denmark.
Phone (+45) 4677 4045, fax (+45) 4677 4046, e-mail nks@catscience.dk, www.nks.org.